bioRxiv preprint doi: https://doi.org/10.1101/2020.06.08.140244; this version posted July 30, 2020. The copyright holder for this preprint (which was not certified by peer review) is the author/funder. All rights reserved. No reuse allowed without permission.

Cross-sectional evaluation of humoral responses against SARS-CoV-2 Spike

Jérémie Prévost[1,2,*], Romain Gasser[1,2,*], Guillaume Beaudoin-Bussières[1,2,*], Jonathan Richard[1,2*], Ralf Duerr[3*] Annemarie Laumaea[1,2,*], Sai Priya Anand[1,4], Guillaume Goyette[1], Mehdi Benlarbi[1], Shilei Ding[1,2], Halima Medjahed[1], Antoine Lewin[5], Josée Perreault[5], Tony Tremblay[5], Gabrielle Gendron-Lepage[1], Nicolas Gauthier[6], Marc Carrier[7], Diane Marcoux[8], Alain Piché[9], Myriam Lavoie[10], Alexandre Benoit[11], Vilayvong Loungnarath[12], Gino Brochu[13], Elie Haddad[2,15,18], Hannah D. Stacey[19], Matthew S. Miller[19], Marc Desforges[14,15], Pierre J. Talbot[14], Graham T. Gould Maule[16], Marceline Côté[16], Christian Therrien[17], Bouchra Serhir[17], Renée Bazin[5], Michel Roger[1,2,17] and Andrés Finzi[1,2,4,#]

[1]Centre de Recherche du CHUM, QC H2X 0A9, Canada
[2]Département de Microbiologie, Infectiologie et Immunologie, Université de Montréal, Montreal, QC H2X 0A9, Canada
[3]Department of Pathology, New York University School of Medicine, New York, NY 10016, USA
[4]Department of Microbiology and Immunology, McGill University, Montreal, QC H3A 2B4, Canada
[5]Héma-Québec, Affaires Médicales et Innovation, Québec, QC G1V 5C3, Canada
[6]Hôpital Sacré-Cœur de Montréal, Montreal, QC H4J 1C5, Canada
[7]Hôpital Cité-de-la-Santé, Laval, QC H7M 3L9, Canada
[8]Hôtel-Dieu de Lévis, Lévis, QC G6V 3Z1, Canada
[9]Centre Hospitalier Universitaire de Sherbrooke, Sherbrooke, QC J1H 5H4, Canada
[10]CIUSSS du Saguenay-Lac-Saint-Jean, Hôpital de Chicoutimi, Chicoutimi, QC G7H 5H6, Canada
[11]Hôpital de Verdun, Montreal, QC H4G 2A3, Canada
[12]CHU de Québec, Hôpital Enfant-Jésus, Quebec, QC G1J 1Z4, Canada
[13]CIUSSS de la Mauricie-et-du-Centre-du-Québec, Trois-Rivières, QC G9A 5C5, Canada
[14]INRS-Institut Armand Frappier, Laval, QC H7V 1B7, Canada
[15]CHU Ste-Justine, Montreal, QC H3T 1C5, Canada
[16]Department of Biochemistry, Microbiology and Immunology, and Center for Infection, Immunity, and Inflammation, University of Ottawa, Ottawa, ON K1H 8M5, Canada
[17]Laboratoire de Santé Publique du Québec, Institut national de santé publique du Québec, Sainte-Anne-de-Bellevue, QC H9X 3R5, Canada
[18]Département de Pédiatrie, Université de Montréal, Montreal, QC H3T 1C5, Canada
[19] Micheal G. DeGroote Institute for Infectious Disease Research, Master Immunology Research Centre, Department of Biochemistry and Biomedical Sciences, McMaster University, Hamilton, ON L8N 3Z5, Canada

*Contributed equally

[#] Correspondence: andres.finzi@umontreal.ca

Running Title: Antibody responses against SARS-CoV-2 S

bioRxiv preprint doi: https://doi.org/10.1101/2020.06.08.140244; this version posted July 30, 2020. The copyright holder for this preprint (which was not certified by peer review) is the author/funder. All rights reserved. No reuse allowed without permission.

Key Words: Coronavirus, COVID-19, SARS-CoV-2, Spike glycoproteins, RBD, ELISA, IgM, IgG, neutralization, cross-reactivity

Word Count for Abstract: 168

Total Character Count for the Manuscript: 21485

bioRxiv preprint doi: https://doi.org/10.1101/2020.06.08.140244; this version posted July 30, 2020. The copyright holder for this preprint (which was not certified by peer review) is the author/funder. All rights reserved. No reuse allowed without permission.

ABSTRACT

The SARS-CoV-2 virus is responsible for the current worldwide coronavirus disease 2019 (COVID-19) pandemic, infecting millions of people and causing hundreds of thousands of deaths. The Spike glycoprotein of SARS-CoV-2 mediates viral entry and is the main target for neutralizing antibodies. Understanding the antibody response directed against SARS-CoV-2 is crucial for the development of vaccine, therapeutic and public health interventions. Here we performed a cross-sectional study on 106 SARS-CoV-2-infected individuals to evaluate humoral responses against the SARS-CoV-2 Spike. The vast majority of infected individuals elicited anti-Spike antibodies within 2 weeks after the onset of symptoms. The levels of receptor-binding domain (RBD)-specific IgG persisted overtime, while the levels of anti-RBD IgM decreased after symptoms resolution. Some of the elicited antibodies cross-reacted with other human coronaviruses in a genus-restrictive manner. While most of individuals developed neutralizing antibodies within the first two weeks of infection, the level of neutralizing activity was significantly decreased over time. Our results highlight the importance of studying the persistence of neutralizing activity upon natural SARS-CoV-2 infection.

bioRxiv preprint doi: https://doi.org/10.1101/2020.06.08.140244; this version posted July 30, 2020. The copyright holder for this preprint (which was not certified by peer review) is the author/funder. All rights reserved. No reuse allowed without permission.

MAIN

The first step in the replication cycle of coronaviruses is viral entry. This is mediated by their trimeric Spike (S) glycoproteins. Similar to SARS-CoV, the S glycoprotein of SARS-CoV-2 interacts with angiotensin-converting enzyme 2 (ACE2) as its host receptor (Hoffmann et al., 2020; Shang et al., 2020; Walls et al., 2019). During entry, the Spike binds the host cell through interaction between its receptor binding domain (RBD) and ACE2 and is cleaved by cell surface proteases or endosomal cathepsins (Hoffmann et al., 2020; Ou et al., 2020; Zang et al., 2020), triggering irreversible conformational changes in the S protein enabling membrane fusion and viral entry (Walls et al., 2020; Wrapp et al., 2020). The SARS-CoV-2 Spike is very immunogenic, with RBD representing the main target for neutralizing antibodies (Ju et al., 2020; Shi et al., 2020; Wu et al., 2020; Yuan et al., 2020). Humoral responses are important for preventing and controlling viral infections (Murin et al., 2019; Rouse and Sehrawat, 2010). However, little is known about the chronology and durability of the human antibody response against SARS-CoV-2.

Here we analyzed serological samples from 106 SARS-CoV-2-infected individuals at different times post-symptoms onset and 10 uninfected individuals for their reactivity to SARS-CoV-2 Spike glycoprotein, cross-reactivity with other human CoV (HCoV), as well as virus neutralization. Samples were collected from COVID-19 positive individuals starting on March 2020 or healthy individuals before the COVID-19 outbreak (COVID-19 negative). Cross-sectional serum samples (n=79) were collected from individuals presenting typical clinical symptoms of acute SARS-CoV-2 infection (Table 1). All patients were positive for SARS-CoV-2 by RT-PCR on nasopharyngeal specimens. The average age of the infected patients was 55

bioRxiv preprint doi: https://doi.org/10.1101/2020.06.08.140244; this version posted July 30, 2020. The copyright holder for this preprint (which was not certified by peer review) is the author/funder. All rights reserved. No reuse allowed without permission.

years old, including 33 males and 46 females. Samples were classified into 4 different time points after symptoms onset: 24 (11 males, 13 females) were obtained at 2-7 days (T1, median = 3 days), 20 (9 males, 11 females) between 8-14 days (T2, median = 11 days), 27 (10 males, 16 females) between 16-30 days (T3, median = 23 days) and 9 (3 males, 6 females) between 31-43 days (T4, median = 36 days). Samples were also obtained from 27 convalescent patients (20 males, 7 females, median = 41 days), who have been diagnosed with or tested positive for COVID-19 with complete resolution of symptoms for at least 14 days.

We first evaluated the presence of RBD-specific IgG and IgM antibodies by ELISA (Amanat et al., 2020; Stadlbauer et al., 2020). The level of RBD-specific IgM peaked at T2 and was followed by a stepwise decrease over time (T3, T4 and Convalescent) (Figure 1). Three quarter of the patients had detectable anti-RBD IgM two weeks after the onset of the symptoms. Similarly, 85% of patients in T2 developed anti-RBD IgG, reaching 100% in convalescent patients. In contrast to IgM, the levels of RBD-specific IgG peaked at T3 and remained relatively stable after complete resolution of symptoms (convalescent patients).

We next used flow cytometry to examine the ability of sera to recognize the full-length SARS-CoV-2 Spike expressed at the cell surface. Briefly, 293T cells expressing SARS-CoV-2 S glycoproteins were stained with samples, followed by incubation with secondary antibodies recognizing all antibody isotypes (including IgG, IgM and IgA). As presented in Figure 2, 54.2% of the sera from T1 already contained SARS-CoV-2 full Spike-reactive antibodies. Interestingly, the majority of patients from T2, T3, T4 and convalescent groups were found to be seropositive in agreement with previous report (Grzelak et al., 2020). The higher seropositivity detected by

bioRxiv preprint doi: https://doi.org/10.1101/2020.06.08.140244; this version posted July 30, 2020. The copyright holder for this preprint (which was not certified by peer review) is the author/funder. All rights reserved. No reuse allowed without permission.

115 flow cytometry is most likely due to the detection of antibodies of multiple specificity and of
116 different isotypes simultaneously. Antibody levels targeting the SARS-CoV-2 Spike significantly
117 increased from T1 to T2/T3 and remained relatively stable thereafter. As expected, the levels of
118 antibodies recognizing the full Spike correlated with the presence of both RBD-specific IgG and
119 IgM (Figure S1). We also evaluated potential cross-reactivity against the closely related SARS-
120 CoV Spike. None of the COVID-19 negative samples recognized the SARS-CoV Spike. While
121 the reactivity of COVID-19+ samples to SARS-CoV S was lower than for SARS-CoV-2 S, it
122 followed a similar progression and significantly correlated with their reactivity to SARS-CoV-2
123 full Spike or RBD protein (Figure 2 and S1). This indicates that SARS-CoV-2-elicited antibodies
124 cross-react with human *Sarbecoviruses*. This was also observed with another *Betacoronavirus*
125 (OC43) but not with *Alphacoronavirus* (NL63, 229E) S glycoproteins, suggesting a genus-
126 restrictive cross-reactivity (Figure 2C and S1). Of note, anti-OC43 RBD antibodies did not
127 fluctuate upon SARS-CoV-2 infection (Figure S2). Therefore, this differential cross-reactivity
128 could be explained by the high degree of conservation in the S protein fusion machinery,
129 particularly in the S2 subunit among *Betacoronaviruses* (Jaimes et al., 2020; Madu et al., 2009;
130 Zhou et al., 2020).
131
132 We next measured the capacity of patient samples to neutralize pseudoparticles bearing
133 SARS-CoV-2 S, SARS-CoV S or VSV-G glycoproteins using 293T cells stably expressing
134 ACE2 as target cells (Figure 3 and S3). Neutralizing activity, as measured by the neutralization
135 half-maximum inhibitory dilution (ID_{50}) or the neutralization 80% inhibitory dilution (ID_{80}), was
136 detected in most patients within 2 weeks after the onset of symptoms (T2, T3, T4 and
137 Convalescent patients) (Figure 3). SARS-CoV-2 neutralization was specific since no

bioRxiv preprint doi: https://doi.org/10.1101/2020.06.08.140244; this version posted July 30, 2020. The copyright holder for this preprint (which was not certified by peer review) is the author/funder. All rights reserved. No reuse allowed without permission.

neutralization was observed against pseudoparticles expressing VSV-G. The capacity to neutralize SARS-CoV-2 S-pseudotyped particles significantly correlated with the presence of RBD-specific IgG/IgM and anti-S antibodies (Figure S4). While the percentage of patients eliciting neutralizing antibodies against SARS-CoV-2 Spike remained relatively stable 2 weeks after disease symptom onset (T2, T3, T4 and Convalescent patients), neutralizing antibody titers significantly decreased after 1 month of infection (T4) or after the complete resolution of symptoms as observed in the convalescent patients (Figure 3G and 3H). Similarly to RBD-specific IgM, levels of RBD-specific IgA were also found to peak at T2 and decrease over time. However, RBD-specific IgM levels displayed a stronger correlation with neutralization acitivity compared to RBD-specific IgG and IgA, suggesting a more prominent role for IgM, but the decrease in IgA could also contribute to the loss of neutralization activity as recently suggested (Sterlin et al., 2020). Cross-reactive neutralizing antibodies against SARS-CoV S protein (Figure 2B) were also detected in some SARS-CoV-2-infected individuals, but with significantly lower potency and waned over time. We note that around 40% of convalescent patients did not exhibit any neutralizing activity. This suggests that the production of neutralizing antibodies is not a prerequisite to the resolution of the infection and that other arms of the immune system could be sufficient to control the infection in an important proportion of the population.

To determine whether underlying correlation patterns among antibody responses detected in SARS-CoV-2 infected individuals were associated with demographic and clinical parameters, we performed a comprehensive correlation analysis, focusing on data from the acute stages of SARS-CoV-2 infection (T1, T2, T3 and T4) (Figure 4 & S5). This analysis revealed a prominent cluster of positive correlations between SARS-CoV-2, SARS-CoV, and OC43 Spike antibody

bioRxiv preprint doi: https://doi.org/10.1101/2020.06.08.140244; this version posted July 30, 2020. The copyright holder for this preprint (which was not certified by peer review) is the author/funder. All rights reserved. No reuse allowed without permission.

161 binding, SARS-CoV-2 neutralization, and days post-symptoms onset (Figure S5). The cluster
162 became evident in a linear correlation analysis involving all study parameters (Figure S5A). Of
163 interest, clinical parameters formed another cluster of positive correlations between respiratory
164 symptoms, hospitalization, oxygen supplementation and intensive care unit (ICU) admission
165 (Figure S5A). The presence of respiratory symptoms and hospitalization also correlated with age
166 of the infected patients. Studying the network of immunologic and clinical correlation pairs
167 longitudinally (from T1 to T4), we observed an increased diversification of associations between
168 the parameters (Figure 4B-E), Associations between anti-Spike Abs and clinical parameters
169 enhanced overtime and was more prominent 3 weeks after the onset of the symptoms (T3 & T4).
170 Admission to the ICU was significantly associated with levels of RBD-specific IgM and IgG and
171 total SARS-CoV-2 Spike Abs (Figure 4A & S5A). The presence of respiratory symptoms was
172 linked to higher levels of RBD-specific IgM and of neutralization activity against SARS-CoV-2
173 S (Figure 4A). Indeed, neutralizers (patients with detectable neutralization ID_{50} against SARS-
174 CoV-2) were found to have stronger antibody responses and were more inclined to present
175 respiratory symptoms (Figure S6).
176
177 This study helps to better understand the kinetics and persistence of humoral responses
178 directed against SARS-CoV-2 (Figure 1, 2 & 3). Our results reveal that the vast majority of
179 infected individuals are able to elicit antibodies directed against SARS-CoV-2 Spike within 2
180 weeks after symptom onset and persist after the resolution of the infection. Accordingly, all
181 tested convalescent patients were found to be seropositive. As expected, RBD-specific IgM
182 levels decreased over the duration of the study while IgG remained relatively stable. Our results
183 highlight how SARS-CoV-2 Spike, like other coronaviruses, appears to be relatively easily

bioRxiv preprint doi: https://doi.org/10.1101/2020.06.08.140244; this version posted July 30, 2020. The copyright holder for this preprint (which was not certified by peer review) is the author/funder. All rights reserved. No reuse allowed without permission.

recognized by Abs present in sera from infected individuals. This was suggested to be linked to the higher processing of glycans compared to other type I fusion protein, such as HIV-1 Env, Influenza A HA or filoviruses GP (Watanabe et al., 2020a; Watanabe et al., 2020b). The ease of naturally-elicited Abs to recognize the Spike might be associated with the low rate of somatic hypermutation observed in neutralizing Abs (Ju et al., 2020). This low somatic hypermutation rate could in turn explain why the majority of the SARS-CoV-2 infected individuals are able to generate neutralizing antibodies within only two weeks after infection (Figure 3). In contrast, the development of potent neutralizing antibodies against HIV-1 Env usually requires 2-3 years of infection and require a high degree of somatic hypermutation (Sok and Burton, 2018). Nevertheless, in the case of SARS-CoV-2 infection, the neutralization capacity decreases significantly 6 weeks after the onset of symptoms, following a similar trend as anti-RBD IgM (Figure 1 & 3). Interestingly, anti-RBD IgM presented a stronger correlation with neutralization than IgG and IgA (Figure S4A,C), suggesting that at least part of the neutralizing activity is mediated by IgM. The neutralization activity appears to further decrease after the resolution of symptoms as recently reported in a series of longitudinal studies on convalescent patients (Beaudoin-Bussières et al., 2020; Ibarrondo et al., 2020; Long et al., 2020; Perreault et al., 2020; Yin et al., 2020; Zhang et al., 2020). However, it remains unclear whether this reduced level of neutralizing activity would remain sufficient to protect from re-infection.

bioRxiv preprint doi: https://doi.org/10.1101/2020.06.08.140244; this version posted July 30, 2020. The copyright holder for this preprint (which was not certified by peer review) is the author/funder. All rights reserved. No reuse allowed without permission.

AUTHOR CONTRIBUTIONS

J.Prévost, J.R., B.S., R.B., M.R. and A.F. conceived the study. J.Prévost, J.R., A.F. designed experimental approaches; J.Prévost, G.B.B., R.G., A.Laumaea, J.R., S.P.A., G.G., M.B., S.D., T.T., J.Perreault, A.Lewin., R.D. R.B., M.R., and A.F. performed, analyzed and interpreted the experiments; J.Prévost, G.B.B., J.R., H.M., G.G.-L., H.D.S., M.S.M., M.D., P.T., G.T.G.M., M.Côté and A.F. contributed novel reagents; N.G., M.Carrier, D.M., A.P., M.L., A.B., V.L., G.B., E.H., C.T., R.B. and M.R. collected clinical samples; J.Prévost, J.R. and A.F. wrote the paper. Every author has read edited and approved the final manuscript.

ACKNOWLEDGMENTS

The authors thank the CRCHUM BSL3 and Flow Cytometry Platforms for technical assistance. We thank Dr Florian Krammer (Icahn School of Medicine at Mount Sinai, NY) for the plasmid expressing the SARS-CoV-2 RBD domain, Dr Stefan Pöhlmann (Georg-August University, Germany) for the plasmids coding for SARS-CoV S, SARS-CoV-2 S and HCoV 229E and NL63 S glycoproteins and Dr M. Gordon Joyce (U.S. MHRP) for the monoclonal antibody CR3022. We also thank Danka K Shank and Melina Bélanger Collard from the Laboratoire de Santé Publique du Québec for their help in preparing the specimens. This work was supported by le Ministère de l'Économie et de l'Innovation du Québec, Programme de soutien aux organismes de recherche et d'innovation to A.F and by the Fondation du CHUM. This work was also supported by a CIHR foundation grant #352417 to A.F. Development of SARS-CoV-2 reagents was partially supported by the NIAID Centers of Excellence for Influenza Research and Surveillance (CEIRS) contract HHSN272201400008C. A.F. is the recipient of a Canada Research Chair on Retroviral Entry # RCHS0235 950-232424. R.D. was supported by NIH grant

bioRxiv preprint doi: https://doi.org/10.1101/2020.06.08.140244; this version posted July 30, 2020. The copyright holder for this preprint (which was not certified by peer review) is the author/funder. All rights reserved. No reuse allowed without permission.

R01 AI122953-05. M.C. is the recipient of a Tier II Canada Research Chair in Molecular Virology and Antiviral Therapeutics and an Ontario's Early Researcher Award. J.P., G.B.B. and S.P.A are supported by CIHR fellowships. R.G. is supported by a MITACS Accélération postdoctoral fellowship. M.S.M was supported in part by a CIHR New Investigator Award, and Ontario Early Researcher Award, CIHR COVID Rapid Response Funding, and the W. Garfield Weston Foundation Weston Family Microbiome Initiative. The funders had no role in study design, data collection and analysis, decision to publish, or preparation of the manuscript.

COMPETING INTERESTS

The authors declare no competing interests.

bioRxiv preprint doi: https://doi.org/10.1101/2020.06.08.140244; this version posted July 30, 2020. The copyright holder for this preprint (which was not certified by peer review) is the author/funder. All rights reserved. No reuse allowed without permission.

STAR METHODS

Ethics statement

All work was conducted in accordance with the Declaration of Helsinki in terms of informed consent and approval by an appropriate institutional board. In addition, this study was conducted in accordance with the rules and regulations concerning ethical reviews in Quebec, particularly those specified in the Civil Code (http://legisquebec.gouv.qc.ca/fr/ShowDoc/cs/CCQ-1991) and in subsequent IRB practice. Informed Consent was obtained for all participating subjects and the study was approved by Quebec Public health authorities. Convalescent plasmas were obtained from donors who consented to participate in this research project (REB # 2020-004). The donors were recruited by Héma-Québec and met all donor eligibility criteria for routine apheresis plasma donation, plus two additional criteria: previous confirmed COVID-19 infection and complete resolution of symptoms for at least 14 days. Plasma samples from COVID- children were obtained from donors enrolled in a research protocol from CHU Ste-Justine (REB #3195).

Plasmids

The plasmids expressing the human coronavirus Spikes of SARS-CoV-2, SARS-CoV, NL63 and 229E were previously reported (Hoffmann et al., 2020; Hofmann et al., 2005). The OC43 Spike with an N-terminal 3xFlag tag and C-terminal 17 residue deletion was cloned into pCAGGS following amplification of the spike gene from pB-Cyst-3FlagOC43SC17 (kind gift of James M. Rini, University of Toronto, ON, Canada). The plasmid encoding for SARS-CoV-2 S RBD (residues 319-541) fused with a hexahistidine tag was reported elsewhere (Amanat et al., 2020). The sequence for the HCoV OC43 RBD was obtained from the UniProt Protein Database

bioRxiv preprint doi: https://doi.org/10.1101/2020.06.08.140244; this version posted July 30, 2020. The copyright holder for this preprint (which was not certified by peer review) is the author/funder. All rights reserved. No reuse allowed without permission.

(P36334 SPIKE_CVHOC). An N-terminal 13aa signal sequence and a C-terminal His-tag were added for downstream protein purification. Mammalian cell codon optimization was performed using the GenScript GenSmart Codon Optimization Tool. The RBD gene was synthesized by GenScript and cloned into the pcDNA3.1 plasmid between EcoRI and XhoI sites. The vesicular stomatitis virus G (VSV-G)-encoding plasmid (pSVCMV-IN-VSV-G) was previously described (Lodge et al., 1997). The lentiviral packaging plasmids pLP1 and pLP2, coding for HIV-1 gag/pol and rev respectively, were purchased from Invitrogen. The transfer plasmid (pLenti-C-mGFP-P2A-Puro-ACE2) encoding for human angiotensin converting enzyme 2 (ACE2) fused with a mGFP C-terminal tag and a puromycin selection marker was purchased from OriGene.

Cell lines

293T human embryonic kidney cells (obtained from ATCC) were maintained at 37°C under 5% CO_2 in Dulbecco's modified Eagle's medium (DMEM) (Wisent) containing 5% fetal bovine serum (VWR) and 100 µg/ml of penicillin-streptomycin (Wisent). For the generation of 293T cells stably expressing human ACE2, transgenic lentivirus were produced in 293T using a third-generation lentiviral vector system. Briefly, 293T cells were co-transfected with two packaging plasmids (pLP1 and pLP2), an envelope plasmid (pSVCMV-IN-VSV-G) and a lentiviral transfer plasmid coding for human ACE2 (pLenti-C-mGFP-P2A-Puro-ACE2) (OriGene). Forty-eight hours post-transfection, supernatant containing lentiviral particles was used to infect more 293T cells in presence of 5µg/mL polybrene. Stably transduced cells were enriched upon puromycin selection. 293T-ACE2 cells were then cultured in a medium supplemented with 2 µg/ml of puromycin (Sigma).

bioRxiv preprint doi: https://doi.org/10.1101/2020.06.08.140244; this version posted July 30, 2020. The copyright holder for this preprint (which was not certified by peer review) is the author/funder. All rights reserved. No reuse allowed without permission.

Protein expression and purification

FreeStyle 293F cells (Invitrogen) were grown in FreeStyle 293F medium (Invitrogen) to a density of 1 x 106 cells/mL at 37°C with 8 % CO2 with regular agitation (150 rpm). Cells were transfected with a plasmid coding for SARS-CoV-2 S RBD or OC43 S RBD using ExpiFectamine 293 transfection reagent, as directed by the manufacturer (Invitrogen). One week later, cells were pelleted and discarded. Supernatants were filtered using a 0.22 µm filter (Thermo Fisher Scientific). The recombinant RBD proteins were purified by nickel affinity columns, as directed by the manufacturer (Invitrogen). The RBD preparations were dialyzed against phosphate-buffered saline (PBS) and stored in aliquots at -80°C until further use. To assess purity, recombinant proteins were loaded on SDS-PAGE gels and stained with Coomassie Blue. For cell-surface staining, RBD proteins were fluorescently labelled with Alexa Fluor 594 (Invitrogen) according to the manufacturer's protocol.

Sera and antibodies

Sera from SARS-CoV-2-infected and uninfected donors were collected, heat-inactivated for 1 hour at 56 °C and stored at -80°C until ready to use in subsequent experiments. The monoclonal antibodies CR3022 and 4.3E4 were used as positive controls in ELISA assays and were previously described (Desforges et al., 2013; ter Meulen et al., 2006; Tian et al., 2020; Yuan et al., 2020). Horseradish peroxidase (HRP)-conjugated antibody specific for the Fc region of human IgG (Invitrogen), for the Fc region of human IgM (Jackson ImmunoReasearch) or for the Fc region of human IgA (Jackson ImmunoResearch) were used as secondary antibodies to detect sera binding in ELISA experiments. Alexa Fluor-647-conjugated goat anti-human IgG (H+L) Abs (Invitrogen) were used as secondary antibodies to detect sera binding in flow cytometry

bioRxiv preprint doi: https://doi.org/10.1101/2020.06.08.140244; this version posted July 30, 2020. The copyright holder for this preprint (which was not certified by peer review) is the author/funder. All rights reserved. No reuse allowed without permission.

306 experiment. Polyclonal goat anti-ACE2 (R&D systems) and Alexa-Fluor-conjugated donkey
307 anti-goat IgG Abs (Invitrogen) were used to detect cell-surface expression of human ACE2.
308
309 **ELISA assay**
310 Recombinant SARS-CoV-2 S RBD proteins (or OC43 S RBD proteins) (2.5 µg/ml), or bovine
311 serum albumin (BSA) (2.5 µg/ml) as a negative control, were prepared in PBS and were
312 adsorbed to plates (MaxiSorp; Nunc) overnight at 4°C. Coated wells were subsequently blocked
313 with blocking buffer (Tris-buffered saline [TBS] containing 0.1% Tween20 and 2% BSA) for 1h
314 at room temperature. Wells were then washed four times with washing buffer (Tris-buffered
315 saline [TBS] containing 0.1% Tween20). CR3022 mAb (50ng/ml) or sera from SARS-CoV-2-
316 infected or uninfected donors (1/100; 1/250; 1/500; 1/1000; 1/2000; 1/4000) were diluted in
317 blocking buffer and incubated with the RBD-coated wells for 1h at room temperature. Plates
318 were washed four times with washing buffer followed by incubation with secondary Abs (diluted
319 in blocking buffer) for 1h at room temperature, followed by four washes. HRP enzyme activity
320 was determined after the addition of a 1:1 mix of Western Lightning oxidizing and luminol
321 reagents (Perkin Elmer Life Sciences). Light emission was measured with a LB941 TriStar
322 luminometer (Berthold Technologies). Signal obtained with BSA was subtracted for each serum
323 and were then normalized to the signal obtained with CR3022 mAb present in each plate.
324 Alternatively, the signal obtained with each serum on OC43 RBD was normalized with the
325 signal obtained with 4.3E4 mAb present in each plate. The seropositivity threshold was
326 established using the following formula: mean RLU of all COVID-19 negative sera normalized
327 to CR3022 (or 4.3E4) + (3 standard deviations of the mean of all COVID-19 negative sera).
328

bioRxiv preprint doi: https://doi.org/10.1101/2020.06.08.140244; this version posted July 30, 2020. The copyright holder for this preprint (which was not certified by peer review) is the author/funder. All rights reserved. No reuse allowed without permission.

Flow cytometry analysis of cell-surface staining

Using the standard calcium phosphate method, 10µg of Spike expressor and 2µg of a green fluorescent protein (GFP) expressor (pIRES-GFP) was transfected into 2×10^6 293T cells. At 48h post transfection, 293T cells were stained with sera from SARS-CoV-2-infected or uninfected individuals (1:250 dilution). The percentage of transfected cells (GFP+ cells) was determined by gating the living cell population based on the basis of viability dye staining (Aqua Vivid, Invitrogen). Samples were acquired on a LSRII cytometer (BD Biosciences, Mississauga, ON, Canada) and data analysis was performed using FlowJo vX.0.7 (Tree Star, Ashland, OR, USA). The seropositivity threshold was established using the following formula: (mean of all COVID-19 negative sera + (3 standard deviation of the mean of all COVID-19 negative sera) + inter-assay coefficient of variability).

Virus neutralization assay

Target cells were infected with single-round luciferase-expressing lentiviral particles. Briefly, 293T cells were transfected by the calcium phosphate method with the lentiviral vector pNL4.3 R-E- Luc (NIH AIDS Reagent Program) and a plasmid encoding for SARS-CoV-2 Spike, SARS-CoV Spike or VSV-G at a ratio of 5:4. Two days post-transfection, cell supernatants were harvested and stored at –80°C until use. 293T-ACE2 target cells were seeded at a density of 1×10^4 cells/well in 96-well luminometer-compatible tissue culture plates (Perkin Elmer) 24h before infection. Recombinant viruses in a final volume of 100µl were incubated with the indicated sera dilutions (1/50; 1/250; 1/1250; 1/6250; 1/31250) for 1h at 37°C and were then added to the target cells followed by incubation for 48h at 37°C; cells were lysed by the addition of 30µl of passive lysis buffer (Promega) followed by one freeze-thaw cycle. An LB941 TriStar

bioRxiv preprint doi: https://doi.org/10.1101/2020.06.08.140244; this version posted July 30, 2020. The copyright holder for this preprint (which was not certified by peer review) is the author/funder. All rights reserved. No reuse allowed without permission.

luminometer (Berthold Technologies) was used to measure the luciferase activity of each well after the addition of 100µl of luciferin buffer (15mM $MgSO_4$, 15mM KPO_4 [pH 7.8], 1mM ATP, and 1mM dithiothreitol) and 50µl of 1mM d-luciferin potassium salt (Prolume). The neutralization half-maximal inhibitory dilution (ID_{50}) or the neutralization 80% inhibitory dilution (ID_{80}) represents the sera dilution to inhibit 50% or 80% of the infection of 293T-ACE2 cells by recombinant viruses bearing the indicated surface glycoproteins.

Software Scripts and Visualization

Correlograms were generated using the corrplot package in program R and R Studio (R Core Team, 2013; R Studio Team, 2015). Dendrograms were calculated using the dendPlot function and hclust method, or as implemented in the heatmap package in R. Chord diagrams were generated in R and R Studio based on the circlize and ComplexHeatmap package, as recently described. For time series, area graphs were generated using RawGraphs with DensityDesign interpolation and the implemented normalization using vertically un-centered values (Mauri et al., 2017). Forrest plots and calculations of fold change, significance (Mann-Whitney) and adjusted P values (Holm-Sidak) were done using Excel and Prism v8.2.0. The confidence interval of a quotient of two means was calculated based on the Fieller method using GraphPad QuickCalcs.

Statistical analyses

Statistics were analyzed using GraphPad Prism version 8.0.2 (GraphPad, San Diego, CA, (USA). Every data set was tested for statistical normality and this information was used to apply the appropriate (parametric or nonparametric) statistical test. P values <0.05 were considered

bioRxiv preprint doi: https://doi.org/10.1101/2020.06.08.140244; this version posted July 30, 2020. The copyright holder for this preprint (which was not certified by peer review) is the author/funder. All rights reserved. No reuse allowed without permission.

375 significant; significance values are indicated as * P<0.05, ** P<0.01, *** P<0.001, ****
376 P<0.0001. Corrections for multiple comparisons were performed with the Holm-Sidak method.

bioRxiv preprint doi: https://doi.org/10.1101/2020.06.08.140244; this version posted July 30, 2020. The copyright holder for this preprint (which was not certified by peer review) is the author/funder. All rights reserved. No reuse allowed without permission.

REFERENCES

Amanat, F., Stadlbauer, D., Strohmeier, S., Nguyen, T.H.O., Chromikova, V., McMahon, M., Jiang, K., Arunkumar, G.A., Jurczyszak, D., Polanco, J., *et al.* (2020). A serological assay to detect SARS-CoV-2 seroconversion in humans. Nat Med.

Beaudoin-Bussières, G., Laumaea, A., Anand, S.P., Prévost, J., Gasser, R., Goyette, G., Medjahed, H., Perreault, J., Tremblay, T., Lewin, A., *et al.* (2020). Decline of humoral responses against SARS-CoV-2 Spike in convalescent individuals. bioRxiv.

Desforges, M., Desjardins, J., Zhang, C., and Talbot, P.J. (2013). The acetyl-esterase activity of the hemagglutinin-esterase protein of human coronavirus OC43 strongly enhances the production of infectious virus. J Virol *87*, 3097-3107.

Grzelak, L., Temmam, S., Planchais, C., Demeret, C., Huon, C., Guivel, F., Staropoli, I., Chazal, M., Dufloo, J., Planas, D., *et al.* (2020). SARS-CoV-2 serological analysis of COVID-19 hospitalized patients, pauci-symptomatic individuals and blood donors. medRxiv.

Hoffmann, M., Kleine-Weber, H., Schroeder, S., Kruger, N., Herrler, T., Erichsen, S., Schiergens, T.S., Herrler, G., Wu, N.H., Nitsche, A., *et al.* (2020). SARS-CoV-2 Cell Entry Depends on ACE2 and TMPRSS2 and Is Blocked by a Clinically Proven Protease Inhibitor. Cell *181*, 271-280 e278.

Hofmann, H., Pyrc, K., van der Hoek, L., Geier, M., Berkhout, B., and Pohlmann, S. (2005). Human coronavirus NL63 employs the severe acute respiratory syndrome coronavirus receptor for cellular entry. Proc Natl Acad Sci U S A *102*, 7988-7993.

Ibarrondo, F.J., Fulcher, J.A., Goodman-Meza, D., Elliott, J., Hofmann, C., Hausner, M.A., Ferbas, K.G., Tobin, N.H., Aldrovandi, G.M., and Yang, O.O. (2020). Rapid Decay of Anti–SARS-CoV-2 Antibodies in Persons with Mild Covid-19. New England Journal of Medicine.

Jaimes, J.A., Andre, N.M., Chappie, J.S., Millet, J.K., and Whittaker, G.R. (2020). Phylogenetic Analysis and Structural Modeling of SARS-CoV-2 Spike Protein Reveals an Evolutionary Distinct and Proteolytically Sensitive Activation Loop. J Mol Biol *432*, 3309-3325.

Ju, B., Zhang, Q., Ge, J., Wang, R., Sun, J., Ge, X., Yu, J., Shan, S., Zhou, B., Song, S., *et al.* (2020). Human neutralizing antibodies elicited by SARS-CoV-2 infection. Nature.

Lodge, R., Lalonde, J.P., Lemay, G., and Cohen, E.A. (1997). The membrane-proximal intracytoplasmic tyrosine residue of HIV-1 envelope glycoprotein is critical for basolateral targeting of viral budding in MDCK cells. EMBO J *16*, 695-705.

Long, Q.X., Tang, X.J., Shi, Q.L., Li, Q., Deng, H.J., Yuan, J., Hu, J.L., Xu, W., Zhang, Y., Lv, F.J., *et al.* (2020). Clinical and immunological assessment of asymptomatic SARS-CoV-2 infections. Nat Med.

Madu, I.G., Roth, S.L., Belouzard, S., and Whittaker, G.R. (2009). Characterization of a highly conserved domain within the severe acute respiratory syndrome coronavirus spike protein S2 domain with characteristics of a viral fusion peptide. J Virol *83*, 7411-7421.

Mauri, M., Elli, T., Caviglia, G., Uboldi, G., and Azzi, M. (2017). RAWGraphs: A Visualisation Platform to Create Open Outputs. In Proceedings of the 12th Biannual Conference on Italian SIGCHI Chapter (New York, NY: ACM), p. 5.

Murin, C.D., Wilson, I.A., and Ward, A.B. (2019). Antibody responses to viral infections: a structural perspective across three different enveloped viruses. Nat Microbiol *4*, 734-747.

Ou, X., Liu, Y., Lei, X., Li, P., Mi, D., Ren, L., Guo, L., Guo, R., Chen, T., Hu, J., *et al.* (2020). Characterization of spike glycoprotein of SARS-CoV-2 on virus entry and its immune cross-reactivity with SARS-CoV. Nat Commun *11*, 1620.

bioRxiv preprint doi: https://doi.org/10.1101/2020.06.08.140244; this version posted July 30, 2020. The copyright holder for this preprint (which was not certified by peer review) is the author/funder. All rights reserved. No reuse allowed without permission.

Perreault, J., Tremblay, T., Fournier, M.-J., Drouin, M., Beaudoin-Bussières, G., Prévost, J., Lewin, A., Bégin, P., Finzi, A., and Bazin, R. (2020). Longitudinal analysis of the humoral response to SARS-CoV-2 spike RBD in convalescent plasma donors. bioRxiv.

R Core Team (2013). R: A language and environment for statistical computing. In R Foundation for Statistical Computing (Vienna, Austria).

R Studio Team (2015). RStudio: Integrated Development for R. RStudio, Inc. (Boston, MA).

Rouse, B.T., and Sehrawat, S. (2010). Immunity and immunopathology to viruses: what decides the outcome? Nat Rev Immunol *10*, 514-526.

Shang, J., Ye, G., Shi, K., Wan, Y., Luo, C., Aihara, H., Geng, Q., Auerbach, A., and Li, F. (2020). Structural basis of receptor recognition by SARS-CoV-2. Nature.

Shi, R., Shan, C., Duan, X., Chen, Z., Liu, P., Song, J., Song, T., Bi, X., Han, C., Wu, L., *et al.* (2020). A human neutralizing antibody targets the receptor binding site of SARS-CoV-2. Nature.

Sok, D., and Burton, D.R. (2018). Recent progress in broadly neutralizing antibodies to HIV. Nat Immunol *19*, 1179-1188.

Stadlbauer, D., Amanat, F., Chromikova, V., Jiang, K., Strohmeier, S., Arunkumar, G.A., Tan, J., Bhavsar, D., Capuano, C., Kirkpatrick, E., *et al.* (2020). SARS-CoV-2 Seroconversion in Humans: A Detailed Protocol for a Serological Assay, Antigen Production, and Test Setup. Curr Protoc Microbiol *57*, e100.

Sterlin, D., Mathian, A., Miyara, M., Mohr, A., Anna, F., Claer, L., Quentric, P., Fadlallah, J., Ghillani, P., Gunn, C., *et al.* (2020). IgA dominates the early neutralizing antibody response to SARS-CoV-2. medRxiv.

ter Meulen, J., van den Brink, E.N., Poon, L.L., Marissen, W.E., Leung, C.S., Cox, F., Cheung, C.Y., Bakker, A.Q., Bogaards, J.A., van Deventer, E., *et al.* (2006). Human monoclonal antibody combination against SARS coronavirus: synergy and coverage of escape mutants. PLoS Med *3*, e237.

Tian, X., Li, C., Huang, A., Xia, S., Lu, S., Shi, Z., Lu, L., Jiang, S., Yang, Z., Wu, Y., *et al.* (2020). Potent binding of 2019 novel coronavirus spike protein by a SARS coronavirus-specific human monoclonal antibody. Emerg Microbes Infect *9*, 382-385.

Walls, A.C., Park, Y.J., Tortorici, M.A., Wall, A., McGuire, A.T., and Veesler, D. (2020). Structure, Function, and Antigenicity of the SARS-CoV-2 Spike Glycoprotein. Cell *181*, 281-292 e286.

Walls, A.C., Xiong, X., Park, Y.J., Tortorici, M.A., Snijder, J., Quispe, J., Cameroni, E., Gopal, R., Dai, M., Lanzavecchia, A., *et al.* (2019). Unexpected Receptor Functional Mimicry Elucidates Activation of Coronavirus Fusion. Cell *176*, 1026-1039 e1015.

Watanabe, Y., Allen, J.D., Wrapp, D., McLellan, J.S., and Crispin, M. (2020a). Site-specific glycan analysis of the SARS-CoV-2 spike. Science.

Watanabe, Y., Berndsen, Z.T., Raghwani, J., Seabright, G.E., Allen, J.D., Pybus, O.G., McLellan, J.S., Wilson, I.A., Bowden, T.A., Ward, A.B., *et al.* (2020b). Vulnerabilities in coronavirus glycan shields despite extensive glycosylation. Nat Commun *11*, 2688.

Wrapp, D., Wang, N., Corbett, K.S., Goldsmith, J.A., Hsieh, C.L., Abiona, O., Graham, B.S., and McLellan, J.S. (2020). Cryo-EM structure of the 2019-nCoV spike in the prefusion conformation. Science *367*, 1260-1263.

Wu, Y., Wang, F., Shen, C., Peng, W., Li, D., Zhao, C., Li, Z., Li, S., Bi, Y., Yang, Y., *et al.* (2020). A noncompeting pair of human neutralizing antibodies block COVID-19 virus binding to its receptor ACE2. Science.

bioRxiv preprint doi: https://doi.org/10.1101/2020.06.08.140244; this version posted July 30, 2020. The copyright holder for this preprint (which was not certified by peer review) is the author/funder. All rights reserved. No reuse allowed without permission.

467 Yin, S., Tong, X., Huang, A., Shen, H., Li, Y., Liu, Y., Wu, C., Huang, R., and Chen, Y. (2020).
468 Longitudinal anti-SARS-CoV-2 antibody profile and neutralization activity of a COVID-19
469 patient. J Infect.
470 Yuan, M., Wu, N.C., Zhu, X., Lee, C.D., So, R.T.Y., Lv, H., Mok, C.K.P., and Wilson, I.A.
471 (2020). A highly conserved cryptic epitope in the receptor binding domains of SARS-CoV-2 and
472 SARS-CoV. Science *368*, 630-633.
473 Zang, R., Gomez Castro, M.F., McCune, B.T., Zeng, Q., Rothlauf, P.W., Sonnek, N.M., Liu, Z.,
474 Brulois, K.F., Wang, X., Greenberg, H.B., *et al.* (2020). TMPRSS2 and TMPRSS4 promote
475 SARS-CoV-2 infection of human small intestinal enterocytes. Sci Immunol *5*.
476 Zhang, G., Nie, S., Zhang, Z., and Zhang, Z. (2020). Longitudinal Change of Severe Acute
477 Respiratory Syndrome Coronavirus 2 Antibodies in Patients with Coronavirus Disease 2019. J
478 Infect Dis *222*, 183-188.
479 Zhou, H., Chen, X., Hu, T., Li, J., Song, H., Liu, Y., Wang, P., Liu, D., Yang, J., Holmes, E.C.,
480 *et al.* (2020). A Novel Bat Coronavirus Closely Related to SARS-CoV-2 Contains Natural
481 Insertions at the S1/S2 Cleavage Site of the Spike Protein. Curr Biol.
482

bioRxiv preprint doi: https://doi.org/10.1101/2020.06.08.140244; this version posted July 30, 2020. The copyright holder for this preprint (which was not certified by peer review) is the author/funder. All rights reserved. No reuse allowed without permission.

Figure Legends

Table 1. Cross-sectional SARS-CoV-2 cohort clinical characteristics

Figure 1. Detection of SARS-CoV-2 RBD-specific IgM and IgG over time.

Indirect ELISA was performed using recombinant SARS-CoV-2 RBD and incubated with samples from COVID-19 negative or COVID-19 positive patients at different times after symptoms onset (T1, T2, T3, T4, Convalescent). Anti-RBD binding was detected using (A-C) anti-IgM-HRP or (D-F) anti-IgG-HRP. Relative light units (RLU) obtained with BSA (negative control) were subtracted and further normalized to the signal obtained with the anti-RBD CR3022 mAb present in each plate. Data in graphs (A, D) represent RLU done in quadruplicate. Curves depicted in (B, E) represent the mean RLU detected with all samples from the same group. Undetectable measures are represented as white symbols and limits of detection are plotted. (C, F) Areas under the curve (AUC) were calculated based on RLU datasets shown in (A, D) using GraphPad Prism software. Statistical significance was tested using Kruskal-Wallis tests with a Dunn's post-test (* $p < 0.05$; ** $p < 0.01$; *** $p < 0.001$; **** $p < 0.0001$).

Figure 2. SARS-CoV-2 infection elicits cross-reactive antibodies against other human *Betacoronaviruses*.

Cell-surface staining of 293T cells expressing full-length Spike (S) from different HCoV (A) SARS-CoV-2, (B) SARS-CoV, (C) OC43, NL63 and 229E with samples from COVID-19 negative or COVID-19 positive patients at different stage of infection (T1, T2, T3, T4, Convalescent). The graphs shown represent the median fluorescence intensities (MFI). Undetectable measures are represented as white symbols and limits of detection are plotted.

bioRxiv preprint doi: https://doi.org/10.1101/2020.06.08.140244; this version posted July 30, 2020. The copyright holder for this preprint (which was not certified by peer review) is the author/funder. All rights reserved. No reuse allowed without permission.

Error bars indicate means ± SEM. Statistical significance was tested using Kruskal-Wallis tests with a Dunn's post-test (* $p < 0.05$; ** $p < 0.01$; *** $p < 0.001$; **** $p < 0.0001$).

Figure 3. Anti-Spike neutralizing antibody titers decrease over time.

Pseudoviral particles coding for the luciferase reporter gene and bearing the following glycoproteins: (A, D, G, H) SARS-CoV-2 S, (B, E, I) SARS-CoV S or (C, F) VSV-G were used to infect 293T-ACE2 cells. Pseudoviruses were incubated with serial dilutions of samples from COVID-19 negative or COVID-19 positive patients (T1, T2, T3, T4, Convalescent) at 37°C for 1h prior to infection of 293T-ACE2 cells. Infectivity at each dilution was assessed in duplicate and is shown as the percentage of infection without sera for each glycoprotein. (G, I) Neutralization half maximal inhibitory serum dilution (ID_{50}) and (H) ID_{80} values were determined using a normalized non-linear regression using Graphpad Prism software. Undetectable measures are represented as white symbols. Neutralizer represent patients with (G, I) an ID_{50} over 100 or (H) an ID_{80}. Statistical significance was tested using Mann-Whitney U tests (* $p < 0.05$; ** $p < 0.01$).

Figure 4. Association between clinical and serological parameters in SARS-CoV-2-infected patients.

Chord diagram illustrating the network of linear correlations among nine major serological and clinical factors for (A) all acutely infected individuals (T1, T2, T3 and T4) or (B-E) at different time points. Chords are color-coded according to the magnitude of the correlation coefficient (r); chord width inversely corresponds to the P-value. Asterisks indicate all statistically significant correlations within chords (*$P < 0.05$, **$P < 0.01$, ***$P < 0.005$). (A-E) Correlation analysis was done using nonparametric Spearman rank tests. P-values were adjusted for multiple comparisons

bioRxiv preprint doi: https://doi.org/10.1101/2020.06.08.140244; this version posted July 30, 2020. The copyright holder for this preprint (which was not certified by peer review) is the author/funder. All rights reserved. No reuse allowed without permission.

529 using Holm-Sidak ($\alpha = 0.05$). Statistical comparisons of two parameters were done using Mann-

530 Whitney U tests.

531

bioRxiv preprint doi: https://doi.org/10.1101/2020.06.08.140244; this version posted July 30, 2020. The copyright holder for this preprint (which was not certified by peer review) is the author/funder. All rights reserved. No reuse allowed without permission.

Table 1. Cross-sectional SARS-CoV-2 cohort

Group	n	Days after onset of symptoms (median; day range)	Age (median; age range)	Gender	
				Male (n)	Female (n)
T1	24	3 (2-7)	50 (31-94)	11	13
T2	20	11 (8-14)	64 (34-90)	9	11
T3	26	22 (16-30)	40 (20-93)	10	16
T4	9	36 (31-43)	39 (24-87)	3	6
Convalescent	27	41 (23-52)	37 (19-69)	20	7

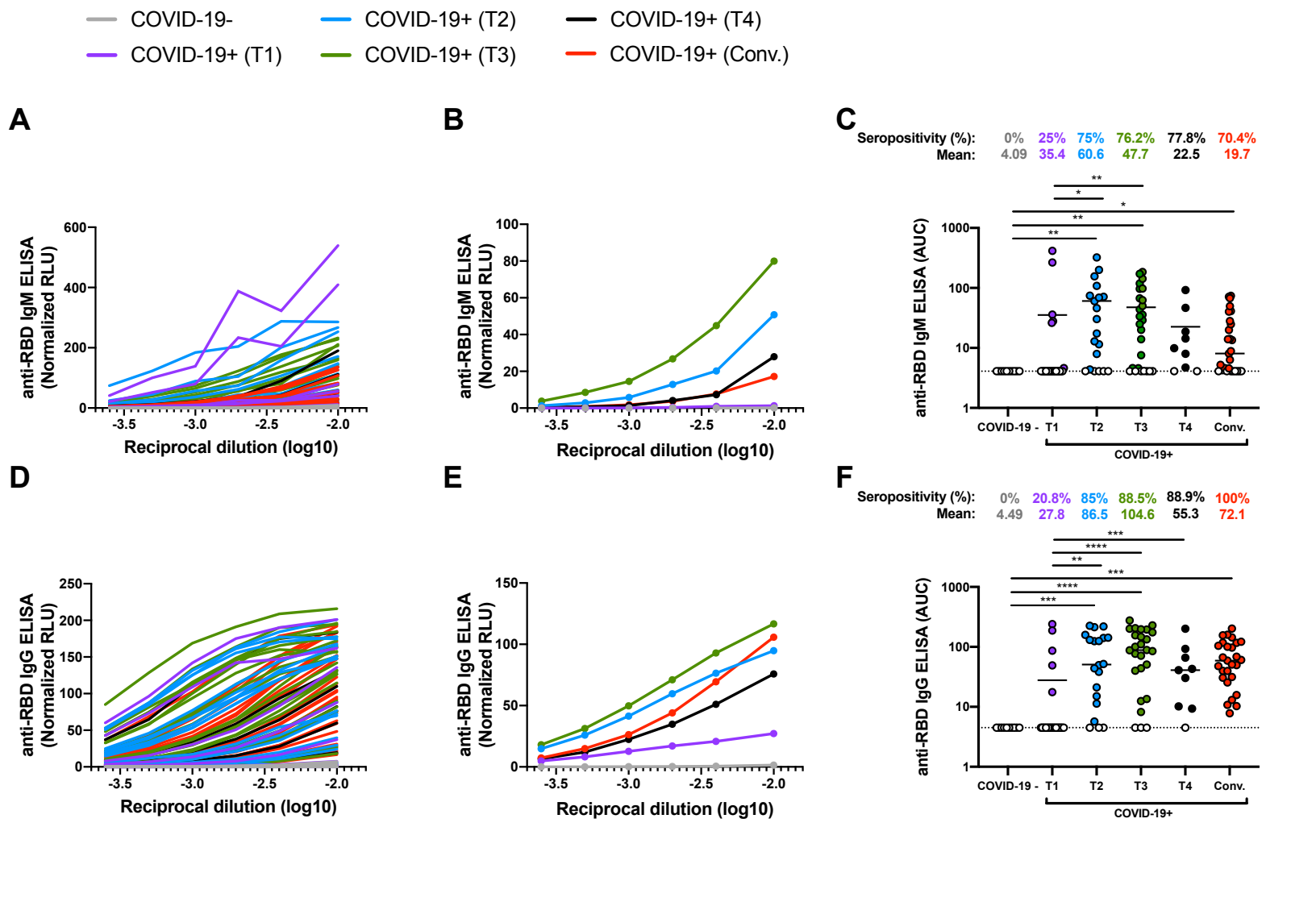
COVID-19-
COVID-19+ (T1)
COVID-19+ (T2)
COVID-19+ (T3)
COVID-19+ (T4)
COVID-19+ (Conv.)
A
anti-RBD IgM ELISA (Normalized RLU)
Reciprocal dilution (log10)
B
anti-RBD IgM ELISA (Normalized RLU)
Reciprocal dilution (log10)
C
Seropositivity (%): 0% 25% 75% 76.2% 77.8% 70.4%
Mean: 4.09 35.4 60.6 47.7 22.5 19.7
anti-RBD IgM ELISA (AUC)
COVID-19 - T1 T2 T3 T4 Conv.
COVID-19+
D
anti-RBD IgG ELISA (Normalized RLU)
Reciprocal dilution (log10)
E
anti-RBD IgG ELISA (Normalized RLU)
Reciprocal dilution (log10)
F
Seropositivity (%): 0% 20.8% 85% 88.5% 88.9% 100%
Mean: 4.49 27.8 86.5 104.6 55.3 72.1
anti-RBD IgG ELISA (AUC)
COVID-19 - T1 T2 T3 T4 Conv.
COVID-19+

A

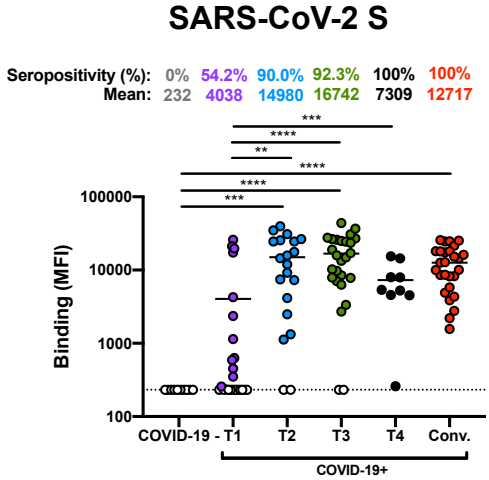
SARS-CoV-2 S
Seropositivity (%): 0% 54.2% 90.0% 92.3% 100% 100%
Mean: 232 4038 14980 16742 7309 12717
Binding (MFI)
100000
10000
1000
100
COVID-19 - T1
T2
T3
T4
Conv.
COVID-19+

B

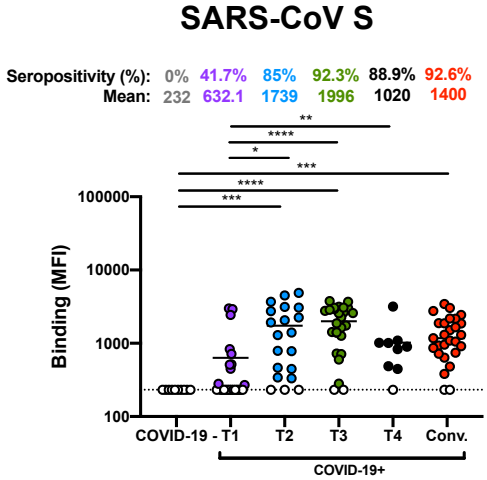
SARS-CoV S
Seropositivity (%): 0% 41.7% 85% 92.3% 88.9% 92.6%
Mean: 232 632.1 1739 1996 1020 1400
Binding (MFI)
100000
10000
1000
100
COVID-19 - T1
T2
T3
T4
Conv.
COVID-19+

C

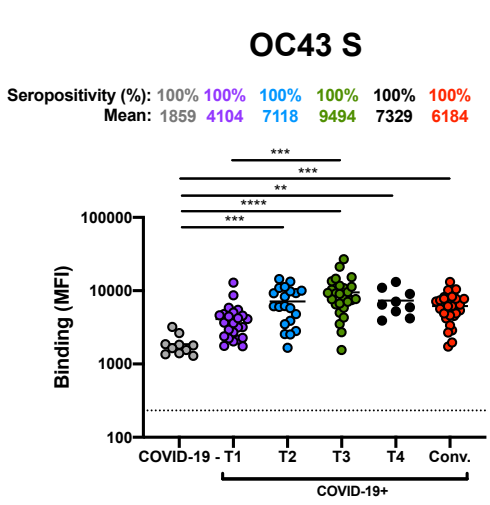
OC43 S
Seropositivity (%): 100% 100% 100% 100% 100% 100%
Mean: 1859 4104 7118 9494 7329 6184
Binding (MFI)
100000
10000
1000
100
COVID-19 - T1
T2
T3
T4
Conv.
COVID-19+

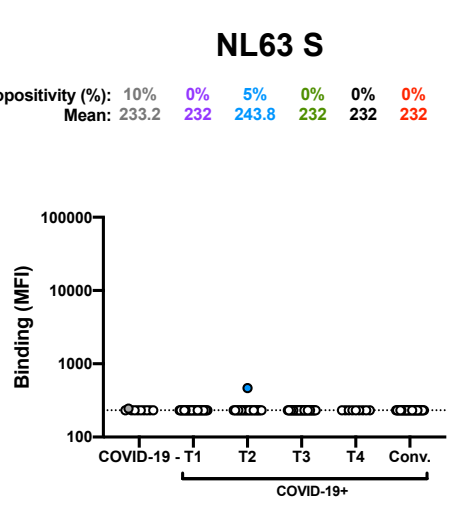
NL63 S
Seropositivity (%): 10% 0% 5% 0% 0% 0%
Mean: 233.2 232 243.8 232 232 232
Binding (MFI)
100000
10000
1000
100
COVID-19 - T1
T2
T3
T4
Conv.
COVID-19+

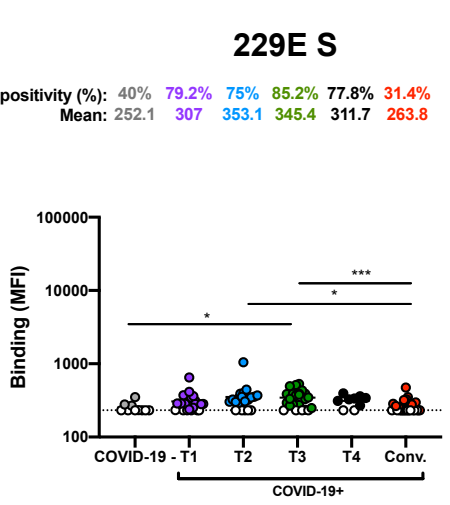
229E S
Seropositivity (%): 40% 79.2% 75% 85.2% 77.8% 31.4%
Mean: 252.1 307 353.1 345.4 311.7 263.8
Binding (MFI)
100000
10000
1000
100
COVID-19 - T1
T2
T3
T4
Conv.
COVID-19+

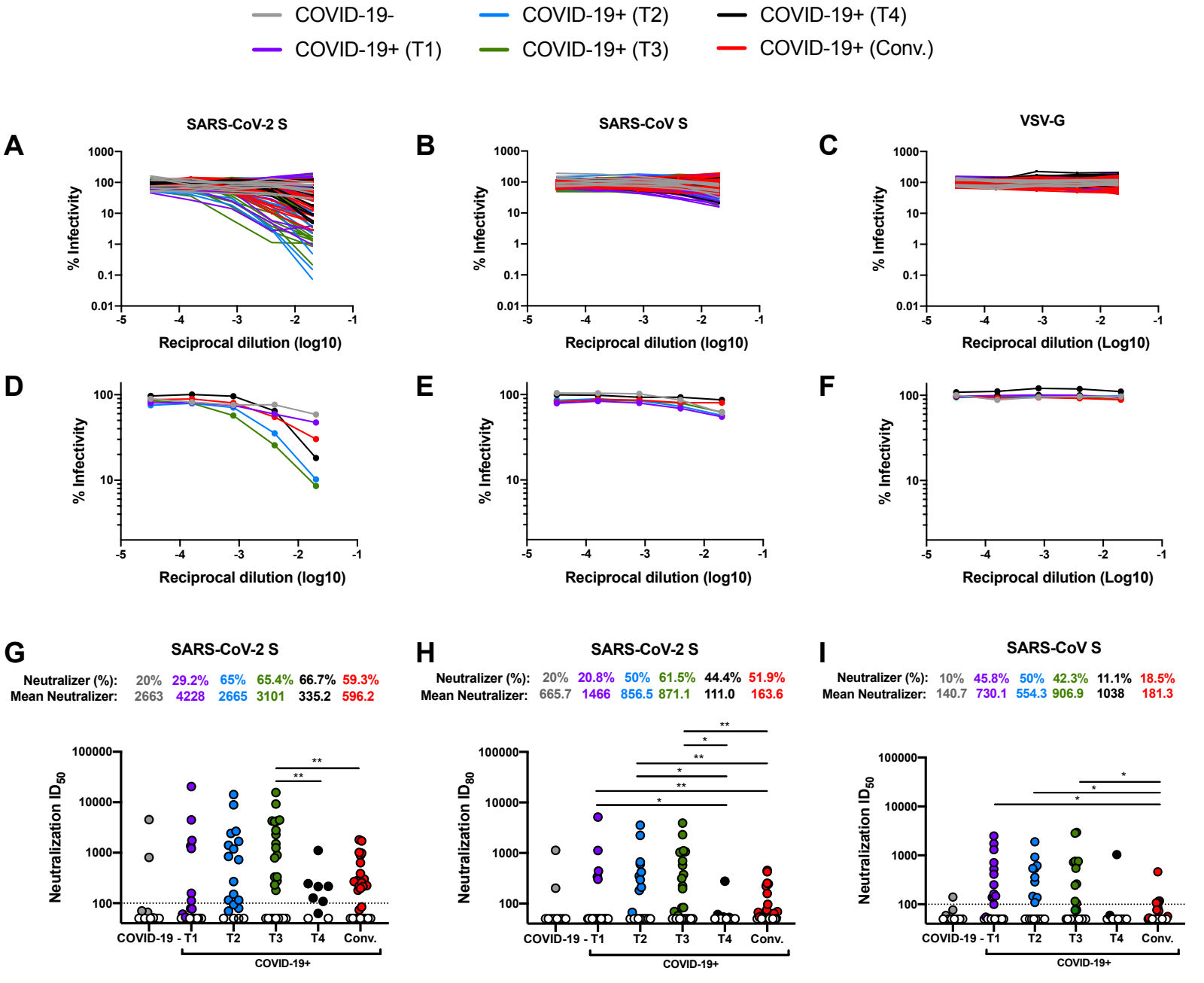
COVID-19-
COVID-19+ (T1)
COVID-19+ (T2)
COVID-19+ (T3)
COVID-19+ (T4)
COVID-19+ (Conv.)
A
SARS-CoV-2 S
B
SARS-CoV S
C
VSV-G
% Infectivity
Reciprocal dilution (log10)
Reciprocal dilution (Log10)
D
E
F
G
SARS-CoV-2 S
Neutralizer (%): 20% 29.2% 65% 65.4% 66.7% 59.3%
Mean Neutralizer: 2663 4228 2665 3101 335.2 596.2
H
SARS-CoV-2 S
Neutralizer (%): 20% 20.8% 50% 61.5% 44.4% 51.9%
Mean Neutralizer: 665.7 1466 856.5 871.1 111.0 163.6
I
SARS-CoV S
Neutralizer (%): 10% 45.8% 50% 42.3% 11.1% 18.5%
Mean Neutralizer: 140.7 730.1 554.3 906.9 1038 181.3
Neutralization ID50
Neutralization ID80
COVID-19 - T1 T2 T3 T4 Conv.
COVID-19+

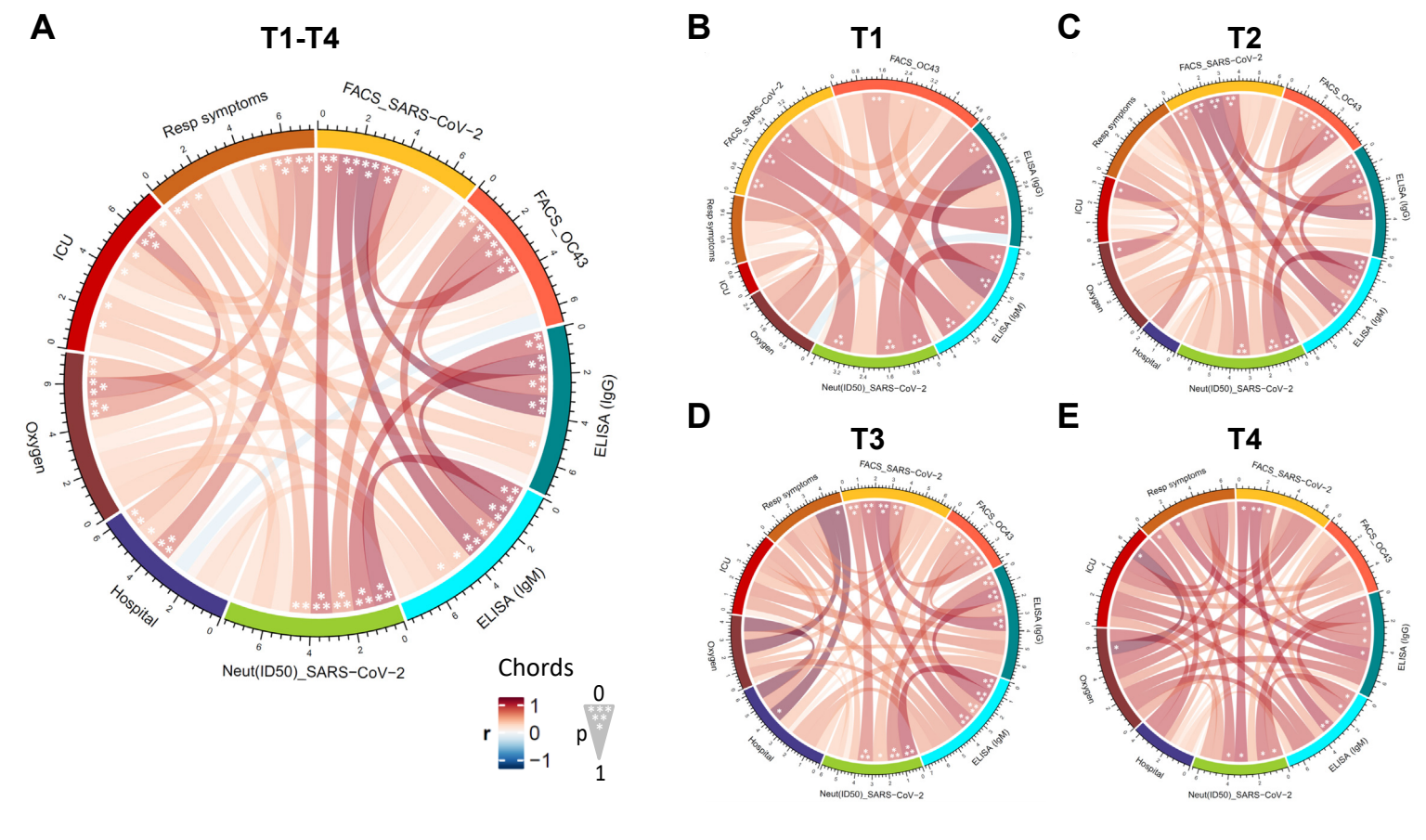
A
T1-T4
Resp symptoms
FACS_SARS-CoV-2
FACS_OC43
ELISA (IgG)
ELISA (IgM)
Neut(ID50)_SARS-CoV-2
Hospital
Oxygen
ICU
Chords
r
1
0
−1
p
0
1
B
T1
C
T2
D
T3
E
T4

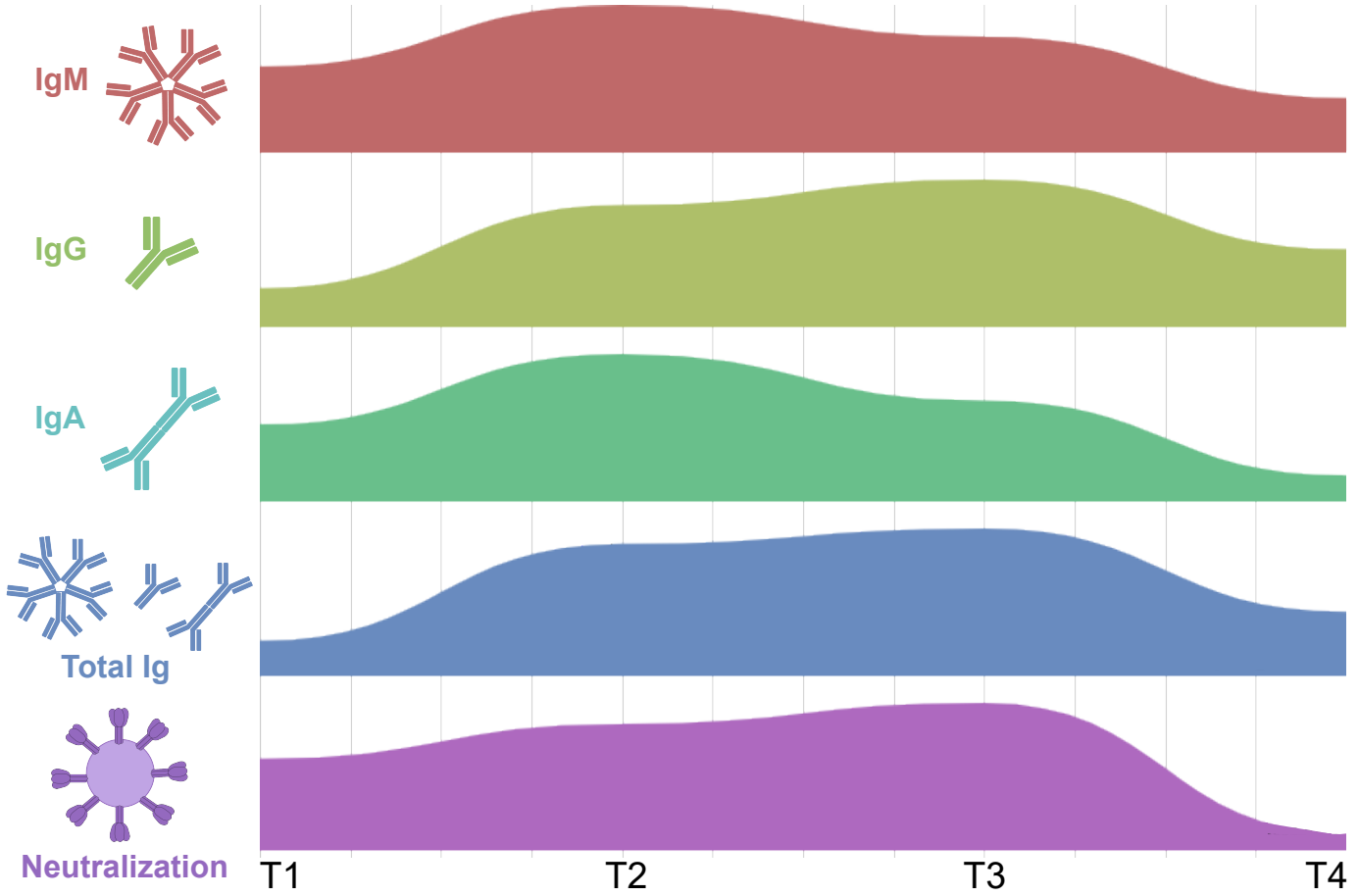
IgM
IgG
IgA
Total Ig
Neutralization
T1
T2
T3
T4

bioRxiv preprint doi: https://doi.org/10.1101/2020.06.08.140244; this version posted July 30, 2020. The copyright holder for this preprint (which was not certified by peer review) is the author/funder. All rights reserved. No reuse allowed without permission.

Supplemental Information

Supplemental information includes 1 table and 6 figures, and can be found online.

Supplemental Table 1. Serological analysis of samples from SARS-CoV-2 infected individuals

Supplemental Figure 1. Detection of antibodies against cell-surface expressed SARS-CoV-2 full Spike correlates with RBD-specific IgG and IgM.

(A,C,E,G,I) Levels of recognition of the different human coronavirus Spikes (SARS-CoV-2 S, SARS-CoV, OC43 S, NL63 S, 229E S) evaluated by flow cytometry (Figure 2) were plotted against the levels of anti-RBD IgG and IgM evaluated by indirect ELISA (Figure 1). (B,D,F,H) Levels of recognition of different HCoV Spikes (SARS-CoV, OC43 S, NL63 S, 229E S) evaluated by flow cytometry were plotted against the levels of recognition of SARS-CoV-2 S (also evaluated by flow cytometry). Statistical analysis was performed using Spearman rank correlation tests.

Supplemental Figure 2. Time course of antibodies against OC43 Spike upon SARS-CoV-2 infection.

(A) Cell-surface staining of 293T cells expressing full-length OC43 Spike (S) and (B) indirect ELISA using recombinant OC43 RBD. S-expressing cells or RBD-coated wells were incubated with samples from COVID-19 negative infants and adults or COVID-19 positive patients at different times after symptoms onset (T1, T2, T3, T4, Convalescent). (A) The graphs shown represent the median fluorescence intensities (MFI). Undetectable measures are represented as white symbols and limits of detection are plotted. (B) Anti-RBD binding was detected using anti-IgG-HRP. Relative light units (RLU) obtained with BSA (negative control) were subtracted and

bioRxiv preprint doi: https://doi.org/10.1101/2020.06.08.140244; this version posted July 30, 2020. The copyright holder for this preprint (which was not certified by peer review) is the author/funder. All rights reserved. No reuse allowed without permission.

25 further normalized to the signal obtained with the anti-OC43 RBD 4.3E4 mAb present in each
26 plate. Data in graphs represent RLU done in quadruplicate, with error bars indicating means ±
27 SEM. Undetectable measures are represented as white symbols and limits of detection are plotted.
28 Statistical significance was tested using Kruskal-Wallis tests with a Dunn's post-test (** $P < 0.01$;
29 *** $P < 0.001$; **** $P < 0.0001$).
30
31 **Supplemental Figure 3. Characterization of 293T-ACE2 cell line**
32 Cell-surface staining of 293T cells and 293T stably expressing human ACE2 (293T-ACE2) with
33 (A) polyclonal goat anti-ACE2 or (B) RBD conjugated with Alexa Fluor 594 (RBD-AF594).
34 Shown in (A,B) are histograms depicting representative anti-ACE2 and RBD-AF594 staining. (C)
35 Recombinant pseudovirus expressing luciferase and bearing SARS-CoV-2 or VSV-G
36 glycoproteins were used to infect 293T or 293T-ACE2 and infectivity was quantified by luciferase
37 activity in cell lysate by relative light units (RLU).
38
39 **Supplemental Figure 4. Anti-RBD antibodies positively correlate with neutralization.**
40 (A) The neutralization ID50 with SARS-CoV-2 S was correlated with the levels of anti-RBD IgG
41 and IgM quantified by ELISA or (B) with the level of anti-SARS-CoV-2 S antibodies quantified
42 by flow cytometry. Statistical significance was tested using Spearman rank correlation tests. (B)
43 Indirect ELISA was performed using recombinant SARS-CoV-2 RBD and incubated with samples
44 from COVID-19 negative or COVID-19 positive patients at different times after symptoms onset
45 (T1, T2, T3, T4, Convalescent). Anti-RBD binding was detected using (B) anti-IgA-HRP. Relative
46 light units (RLU) obtained with BSA (negative control) were subtracted and further normalized to
47 the signal obtained with the anti-RBD CR3022 mAb present in each plate. Undetectable measures

bioRxiv preprint doi: https://doi.org/10.1101/2020.06.08.140244; this version posted July 30, 2020. The copyright holder for this preprint (which was not certified by peer review) is the author/funder. All rights reserved. No reuse allowed without permission.

are represented as white symbols and limits of detection are plotted. Statistical significance was tested using Kruskal-Wallis tests with a Dunn's post-test (* $P < 0.05$; ** $P < 0.01$; **** $P < 0.0001$). (C) The levels of anti-RBD IgA were correlated with the neutralization ID_{50} with SARS-CoV-2 S, the level of anti-SARS-CoV-2 S antibodies quantified by flow cytometry and the levels of anti-RBD IgG and IgM quantified by ELISA. Statistical significance was tested using Spearman rank correlation tests.

Supplemental Figure 5. Correlations between serological measurements and clinical outcome.

Correlograms were generated by plotting together all serological and clinical data obtained from acutely infected COVID-19+ patients (T1, T2 and T3), separated by time points (a-c) or all together (d) or using data obtained from convalescent patients (e). Squares are color-coded according to the magnitude of the correlation coefficient (r) and the square dimensions are inversely proportional with the P-values. Red squares represent a positive correlation between two variables and blue squares present negative correlations. Asterisks indicate all statistically significant correlations (*$P < 0.05$, **$P < 0.01$, ***$P < 0.005$). (a-e) Correlation analysis was done using nonparametric Spearman rank tests.

Supplemental Figure 6. Clinical, demographic, and humoral factors associated with increased SARS-CoV-2 neutralization. Forrest plot of the association of SARS-CoV-2 neutralization with selected clinical, demographic, and humoral parameters. The fold change (mean and 95% confidence interval) of the parameters, listed on the y-axis, between neutralizers (ID50 >100) and non-neutralizers (ID50 <100) is displayed on the x-axis. Significance P and

bioRxiv preprint doi: https://doi.org/10.1101/2020.06.08.140244; this version posted July 30, 2020. The copyright holder for this preprint (which was not certified by peer review) is the author/funder. All rights reserved. No reuse allowed without permission.

71 adjusted P values (Holm-Sidak method) are shown in columns to the right. Results with $P<0.05$

72 are highlighted in green.

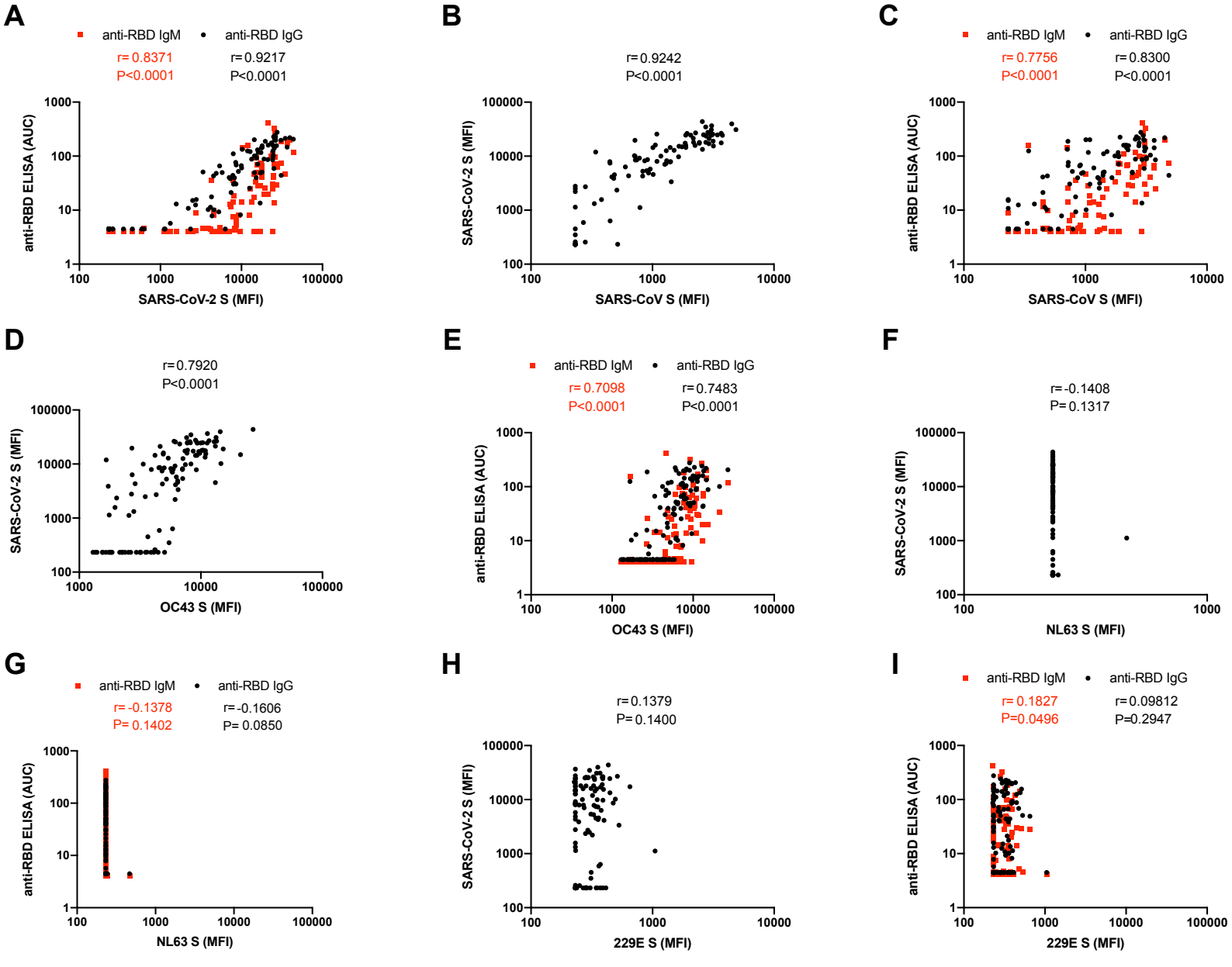
A
anti-RBD IgM
anti-RBD IgG
r= 0.8371
P<0.0001
r= 0.9217
P<0.0001
anti-RBD ELISA (AUC)
SARS-CoV-2 S (MFI)
B
r= 0.9242
P<0.0001
SARS-CoV-2 S (MFI)
SARS-CoV S (MFI)
C
anti-RBD IgM
anti-RBD IgG
r= 0.7756
P<0.0001
r= 0.8300
P<0.0001
anti-RBD ELISA (AUC)
SARS-CoV S (MFI)
D
r= 0.7920
P<0.0001
SARS-CoV-2 S (MFI)
OC43 S (MFI)
E
anti-RBD IgM
anti-RBD IgG
r= 0.7098
P<0.0001
r= 0.7483
P<0.0001
anti-RBD ELISA (AUC)
OC43 S (MFI)
F
r= -0.1408
P= 0.1317
SARS-CoV-2 S (MFI)
NL63 S (MFI)
G
anti-RBD IgM
anti-RBD IgG
r= -0.1378
P= 0.1402
r= -0.1606
P= 0.0850
anti-RBD ELISA (AUC)
NL63 S (MFI)
H
r= 0.1379
P= 0.1400
SARS-CoV-2 S (MFI)
229E S (MFI)
I
anti-RBD IgM
anti-RBD IgG
r= 0.1827
P=0.0496
r= 0.09812
P=0.2947
anti-RBD ELISA (AUC)
229E S (MFI)

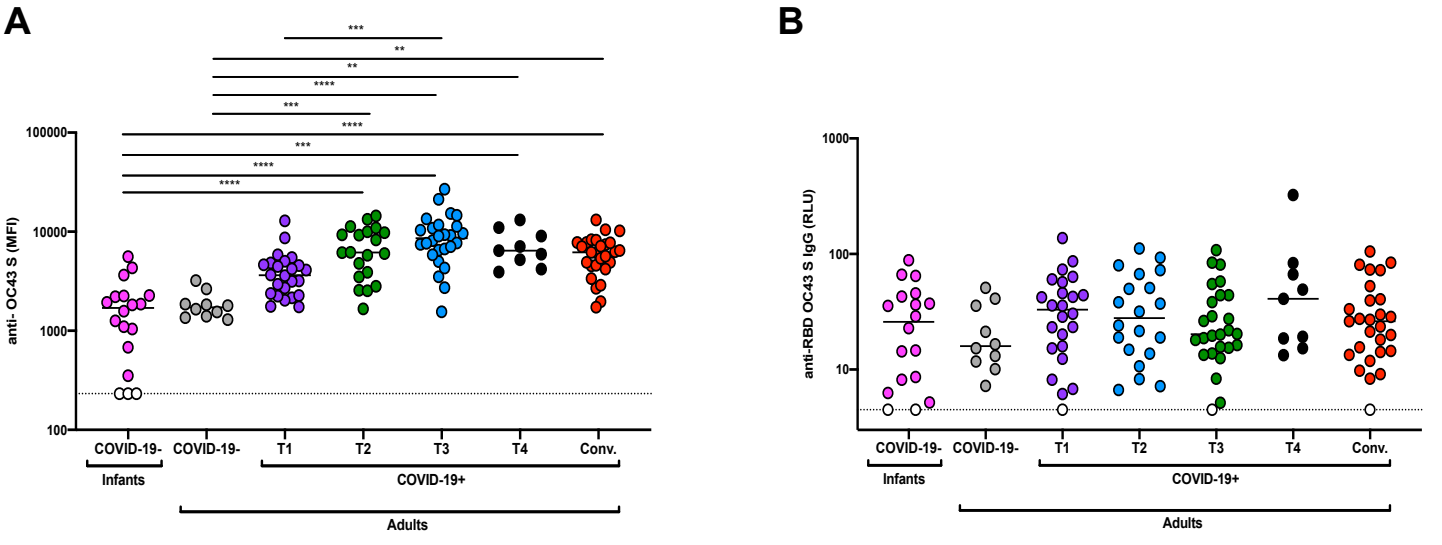
A
B
anti- OC43 S (MFI)
anti-RBD OC43 S IgG (RLU)
100000
10000
1000
100
1000
100
10
***
**
**
****
***
****
***
****
****
COVID-19-
COVID-19-
T1
T2
T3
T4
Conv.
Infants
COVID-19+
Adults

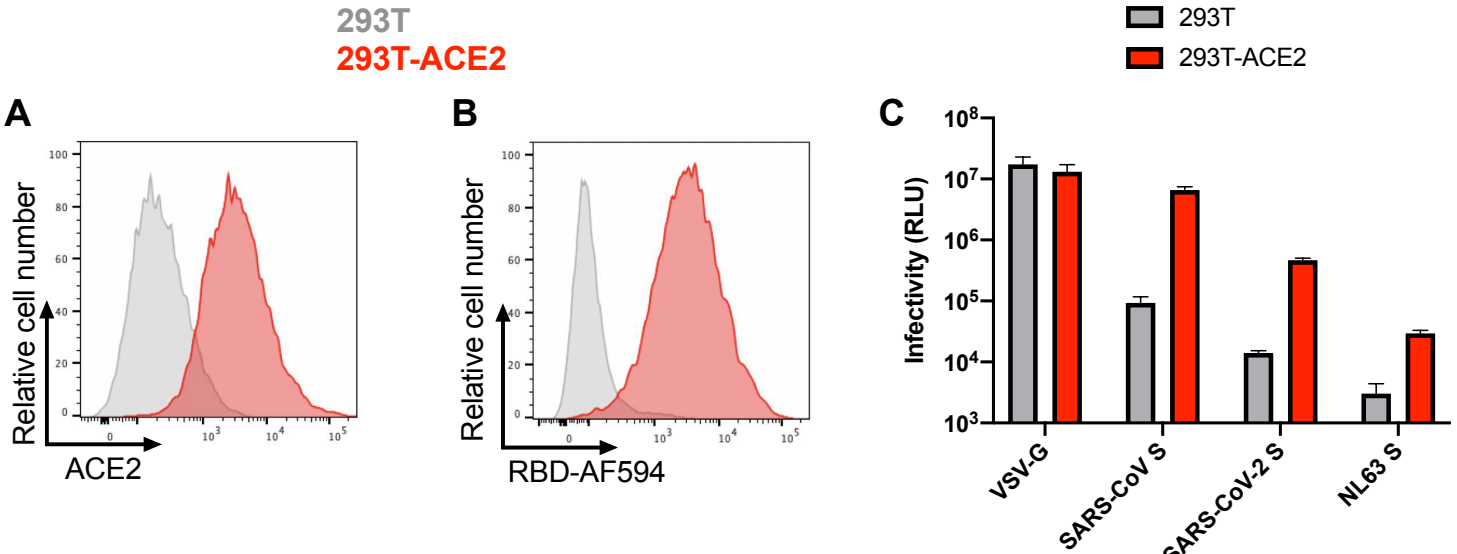
293T
293T-ACE2
A
Relative cell number
ACE2
B
Relative cell number
RBD-AF594
C
293T
293T-ACE2
Infectivity (RLU)
VSV-G
SARS-CoV S
SARS-CoV-2 S
NL63 S

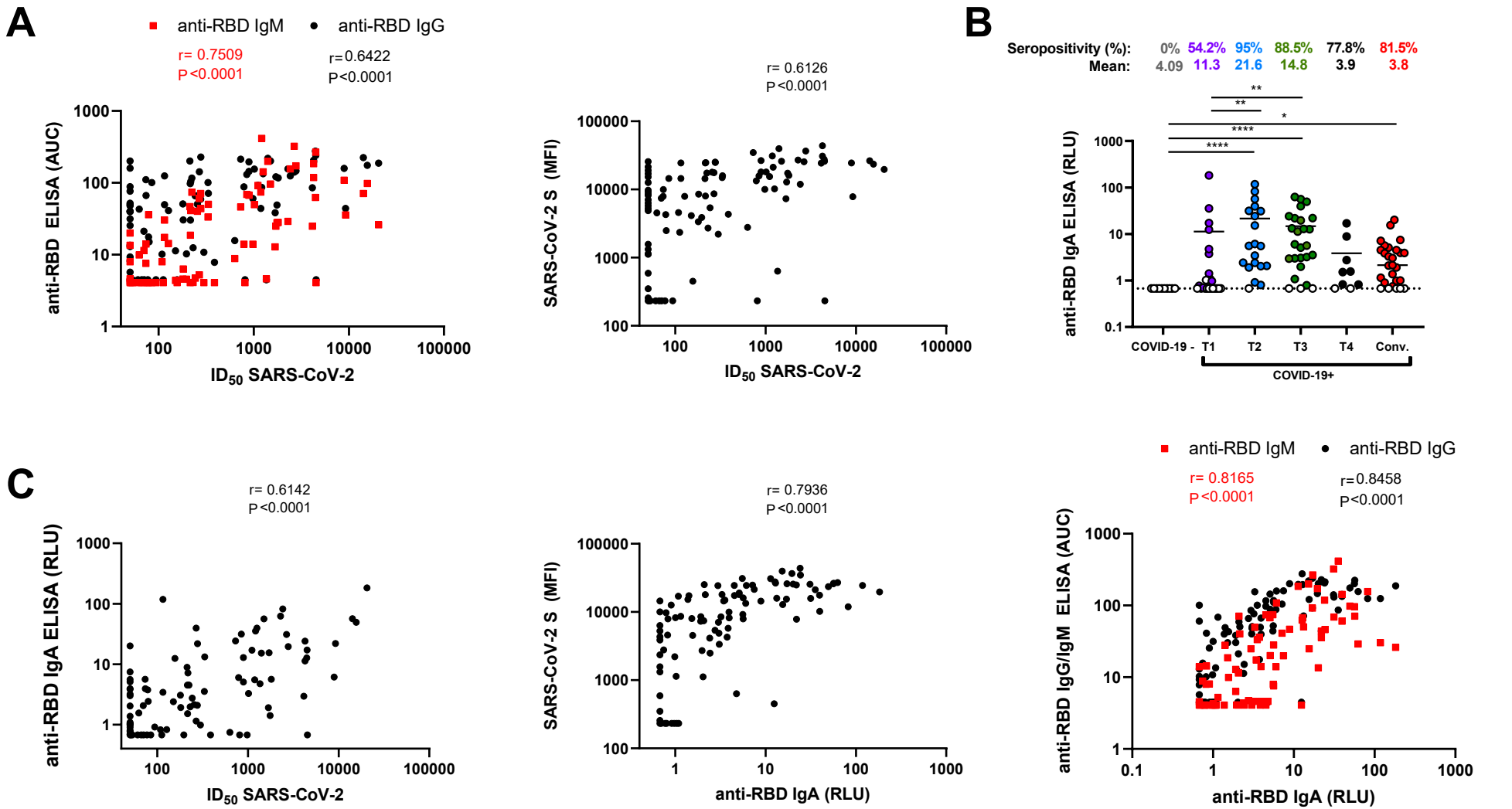
A
anti-RBD IgM
anti-RBD IgG
r= 0.7509
P <0.0001
r=0.6422
P<0.0001
anti-RBD ELISA (AUC)
ID50 SARS-CoV-2
r= 0.6126
P <0.0001
SARS-CoV-2 S (MFI)
ID50 SARS-CoV-2
B
Seropositivity (%): 0% 54.2% 95% 88.5% 77.8% 81.5%
Mean: 4.09 11.3 21.6 14.8 3.9 3.8
anti-RBD IgA ELISA (RLU)
COVID-19 - T1 T2 T3 T4 Conv.
COVID-19+
C
r= 0.6142
P <0.0001
anti-RBD IgA ELISA (RLU)
ID50 SARS-CoV-2
r= 0.7936
P <0.0001
SARS-CoV-2 S (MFI)
anti-RBD IgA (RLU)
anti-RBD IgM
anti-RBD IgG
r= 0.8165
P <0.0001
r=0.8458
P<0.0001
anti-RBD IgG/IgM ELISA (AUC)
anti-RBD IgA (RLU)

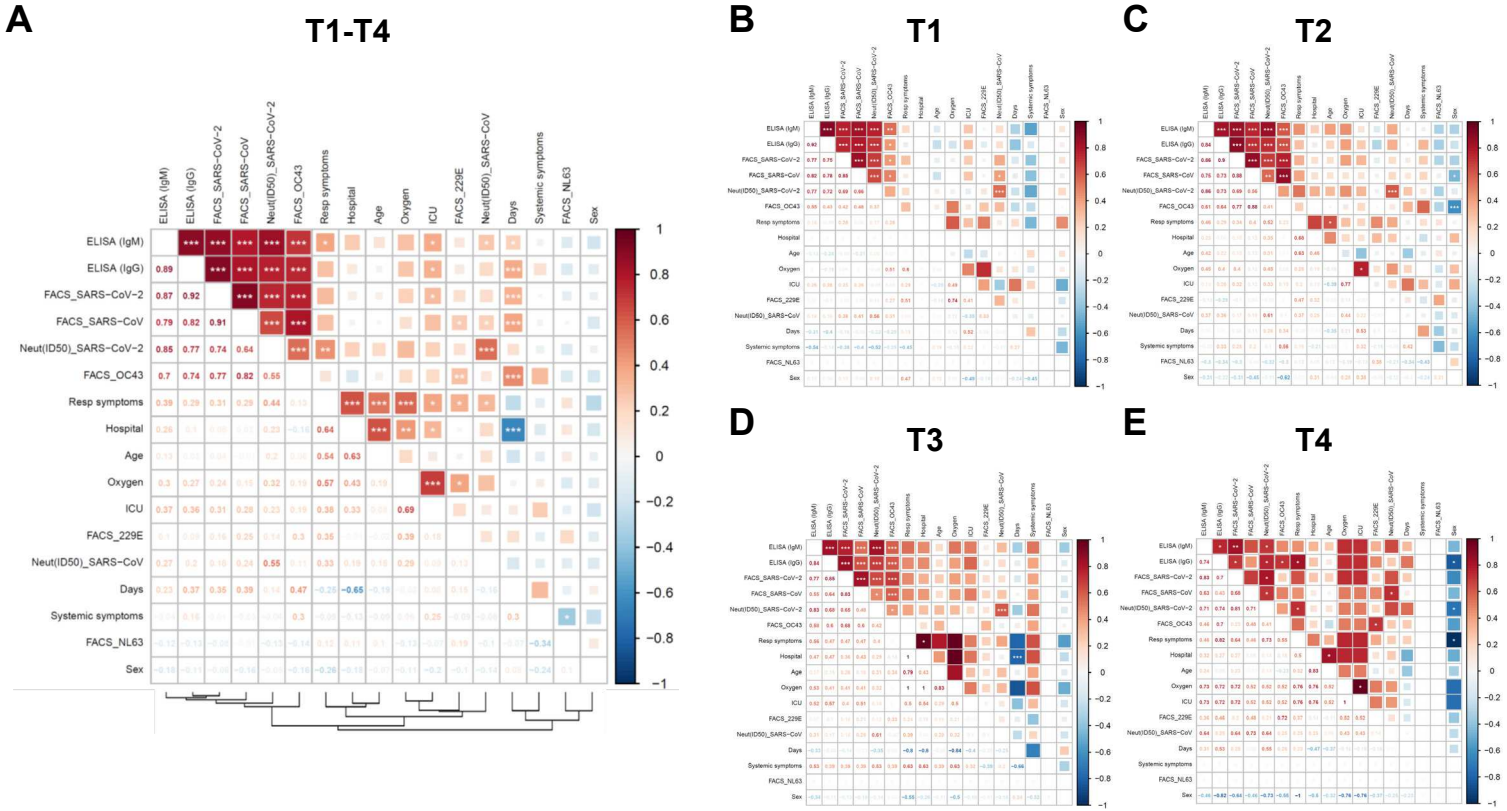
A
T1-T4
B
T1
C
T2
D
T3
E
T4
ELISA (IgM)
ELISA (IgG)
FACS_SARS-CoV-2
FACS_SARS-CoV
Neut(ID50)_SARS-CoV-2
FACS_OC43
Resp symptoms
Hospital
Age
Oxygen
ICU
FACS_229E
Neut(ID50)_SARS-CoV
Days
Systemic symptoms
FACS_NL63
Sex

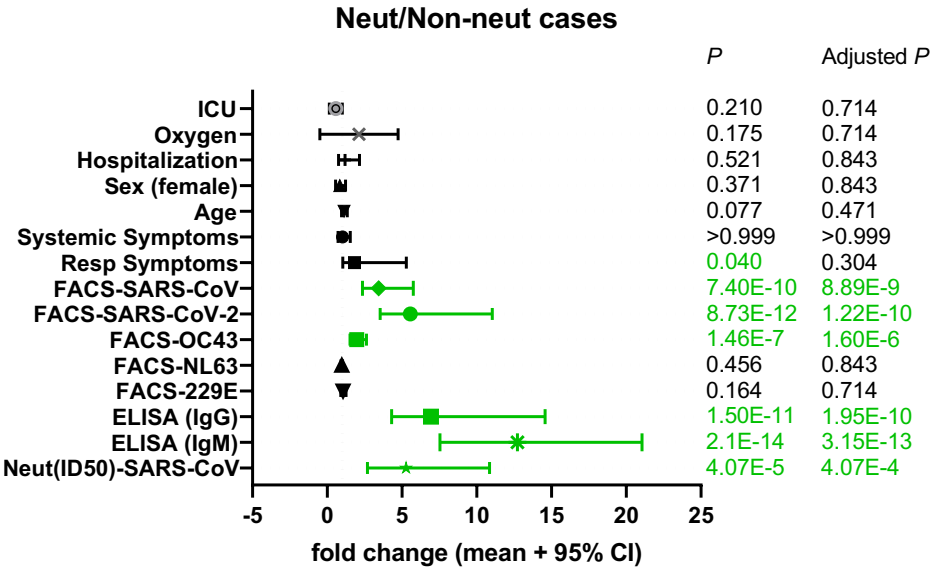
Neut/Non-neut cases
P
Adjusted P
ICU
Oxygen
Hospitalization
Sex (female)
Age
Systemic Symptoms
Resp Symptoms
FACS-SARS-CoV
FACS-SARS-CoV-2
FACS-OC43
FACS-NL63
FACS-229E
ELISA (IgG)
ELISA (IgM)
Neut(ID50)-SARS-CoV
0.210
0.714
0.175
0.714
0.521
0.843
0.371
0.843
0.077
0.471
>0.999
>0.999
0.040
0.304
7.40E-10
8.89E-9
8.73E-12
1.22E-10
1.46E-7
1.60E-6
0.456
0.843
0.164
0.714
1.50E-11
1.95E-10
2.1E-14
3.15E-13
4.07E-5
4.07E-4
-5
0
5
10
15
20
25
fold change (mean + 95% CI)

bioRxiv preprint doi: https://doi.org/10.1101/2020.06.08.140244; this version posted July 30, 2020. The copyright holder for this preprint (which was not certified by peer review) is the author/funder. All rights reserved. No reuse allowed without permission.

Table S1. Serological analysis of samples from COVID-19+ patients

			FACS (MFI)					ELISA (AUC)		Neutralization (ID50)	
Patient ID	Group (T)	Gender	SARS-CoV S	SARS-CoV-2 S	OC43 S	NL63 S	229E S	anti-RBD IgG	anti-RBD IgM	SARS-CoV S	SARS-CoV-2 S
1	T1	F	232	451	3664	232	313	4,49	4,09	250,63	156,47
2	T1	F	232	232	1743	232	232	4,49	4,09	50,00	50,00
3	T1	M	2990	25903	12877	232	284	239,90	266,10	1739,43	4476,28
4	T1	M	831	4270	4831	232	356	17,60	35,98	50,00	78,31
5	T1	F	448	631	5852	232	372	4,49	4,61	524,38	1353,00
6	T1	F	2924	21146	4629	232	227	86,39	415,00	50,00	1211,53
7	T1	F	232	350	5471	232	311	4,49	4,09	54,67	50,00
8	T1	M	232	232	3190	232	232	4,49	4,09	50,00	50,00
9	T1	F	232	232	2152	232	344	4,49	4,09	51,20	60,53
10	T1	F	232	232	4100	232	285	4,49	4,09	50,00	50,00
11	T1	F	2435	17303	8659	232	651	49,05	28,00	1304,97	1752,85
12	T1	M	232	232	3155	232	372	4,49	4,09	50,00	50,00
13	T1	M	232	232	5030	232	285	4,49	4,09	709,22	76,80
14	T1	M	270	590	4557	232	362	4,49	4,09	99,60	50,00
15	T1	F	718	19719	2707	232	232	187,80	26,14	137,97	20533,88
16	T1	M	232	232	2945	232	287	4,49	4,09	50,00	50,00
17	T1	F	232	1140	1762	232	233	4,49	4,09	50,00	50,00
18	T1	F	232	232	4452	232	232	4,49	4,09	50,00	50,00
19	T1	M	517	234	3598	232	283	4,49	4,09	145,33	50,00
20	T1	F	232	232	2270	232	287	4,49	4,09	162,42	52,85
21	T1	M	510	2356	2031	232	281	4,49	4,09	2497,50	111,87
22	T1	M	232	232	2237	232	413	4,49	4,09	147,54	50,00
23	T1	F	280	257	4206	232	251	4,49	4,09	411,52	50,00
24	T1	M	232	232	2380	232	238	4,49	4,09	50,00	50,00
25	T2	F	1399	14478	9308	232	232	49,65	17,40	50,00	115,05
26	T2	M	4493	39640	14425	232	354	219,10	199,40	540,54	1402,52
27	T2	F	332	1325	2810	232	232	5,70	4,09	50,00	50,00
28	T2	F	341	11926	1664	232	321	124,80	155,90	145,48	2412,55
29	T2	M	782	9188	6132	232	232	51,97	7,96	50,00	50,00
30	T2	F	447	7454	4791	232	342	21,14	11,48	50,00	69,88
31	T2	F	2743	34747	8276	232	303	213,50	46,18	50,00	727,27
32	T2	M	3144	25468	9244	232	293	140,80	322,70	287,27	2662,41
33	T2	M	232	232	3888	232	391	4,49	4,09	50,00	50,00
34	T2	M	2067	24488	9993	232	232	158,70	108,50	137,12	8904,72
35	T2	F	790	1122	2563	467	1048	4,49	4,09	50,00	50,00
36	T2	M	3686	17679	10901	232	232	142,40	60,33	921,66	267,67
37	T2	F	1927	26403	6020	232	326	224,40	71,17	1890,72	14178,36
38	T2	F	232	2495	3489	232	302	15,06	4,09	50,00	79,30
39	T2	M	464	4142	6185	232	399	11,33	4,38	614,63	149,99
40	T2	F	2243	15808	9780	232	346	130,50	68,94	108,89	843,17
41	T2	F	1293	7294	5772	232	355	38,45	12,87	356,13	1675,60
42	T2	M	4868	30938	13324	232	370	43,95	74,30	50,00	1184,97
43	T2	F	232	232	2532	232	307	4,49	4,09	540,83	93,37
44	T2	M	3073	24535	11264	232	445	124,90	30,34	50,00	115,31
45	T3	M	3016	25909	8125	232	386	201,50	96,50	260,42	1499,25
46	T3	F	2634	24951	10356	232	332	228,90	43,84	50,00	276,85
47	T3	M	3686	26501	13482	232	391	195,10	67,27	104,66	887,31
48	T3	M	1428	3351	6496	232	529	50,75	4,58	2954,21	179,82
49	T3	M	723	8490	4998	232	232	76,63	4,62	50,00	50,00
50	T3	F	1396	7833	9176	232	330	43,99	35,77	2834,47	9208,10
51	T3	F	1263	7064	5836	232	274	40,10	4,09	50,00	50,00
52	T3	F	2583	13350	10850	232	446	87,89	14,00	244,68	788,02
53	T3	F	3161	19011	15261	232	386	88,59	20,06	50,00	50,00
54	T3	F	2264	27040	11678	232	514	156,50	29,01	76,51	2288,33
55	T3	M	232	232	3511	232	280	4,49	4,09	50,00	50,00
56	T3	F	1747	14934	21177	232	232	100,70	33,47	50,00	329,92
57	T3	F	1641	9732	7461	232	391	8,22	4,09	50,00	50,00
58	T3	F	2575	43788	26862	232	433	205,40	118,80	50,00	4255,32
59	T3	F	281	2714	4297	232	293	12,51	4,12	722,02	229,94
60	T3	F	232	232	1553	232	236	4,49	4,09	75,99	50,00
61	T3	F	2919	17013	9604	232	374	13,49	4,09	50,00	50,00
62	T3	M	1878	15855	7696	232	268	71,25	50,23	50,00	332,23
63	T3	M	711	10219	14607	232	494	133,50	142,70	50,00	1252,98
64	T3	M	3053	30735	7638	232	346	196,80	184,50	114,73	4258,94
65	T3	M	3770	24356	9342	232	390	85,23	24,97	681,20	4123,71
66	T3	M	3067	36647	11330	232	232	147,00	172,40	759,88	2782,42
67	T3	F	2774	23502	6692	232	333	175,20	97,95	755,29	15586,03
68	T3	F	2861	27590	9046	232	232	275,80	62,70	544,37	4444,44
69	T3	F	599	6316	2720	232	378	4,49	4,09	50,00	50,00
70	T3	F	1412	7916	7058	232	249	110,50	7,55	50,00	73,21
71	T4	M	3175	15418	10990	232	395	92,55	92,04	1037,56	1105,22
72	T4	M	1009	14429	9029	232	336	200,70	46,64	50,00	212,59
73	T4	F	487	4529	13163	232	342	42,91	9,91	50,00	62,46
74	T4	F	1089	8002	5933	232	232	30,25	18,67	59,59	215,84
75	T4	M	897	5377	7080	232	311	65,94	4,71	50,00	242,54
76	T4	F	1013	4574	6444	232	360	10,16	7,98	50,00	108,25
77	T4	F	232	260	4186	232	232	4,49	4,09	50,00	50,00
78	T4	F	832	5260	5220	232	327	9,32	4,09	50,00	50,00
79	T4	F	446	7935	3912	232	270	41,04	14,35	50,00	126,79
80	Convalescent	M	2179	18055	7778	232	257	143,90	67,60	50,00	887,31
81	Convalescent	M	232	2775	2685	232	232	15,69	8,86	73,10	631,31
82	Convalescent	M	742	8550	4515	232	232	30,54	6,33	50,00	181,00
83	Convalescent	M	1172	10054	8280	232	265	60,59	13,99	462,11	979,43
84	Convalescent	M	232	2205	6135	232	320	10,82	4,09	76,57	298,42
85	Convalescent	F	3044	25170	7781	232	278	59,04	71,09	50,00	276,40
86	Convalescent	M	1655	15237	4901	232	232	39,86	4,09	50,00	50,00
87	Convalescent	M	911	8625	4588	232	474	68,48	5,22	50,00	267,95
88	Convalescent	M	1056	16116	4911	232	312	117,20	28,04	106,91	1806,68
89	Convalescent	F	864	8202	7062	232	232	39,63	4,60	50,00	50,00
90	Convalescent	M	381	1569	1968	232	232	13,02	4,09	50,00	50,00
91	Convalescent	M	3431	24732	8195	232	232	104,30	41,20	117,27	217,72
92	Convalescent	M	1862	17395	7403	232	232	116,70	73,81	50,00	223,36
93	Convalescent	M	1509	12831	5386	232	232	121,60	24,84	88,57	1706,19
94	Convalescent	M	958	5784	6278	232	232	49,68	4,09	50,00	50,00
95	Convalescent	M	2434	17985	10192	232	284	50,63	40,18	50,00	254,91
96	Convalescent	M	2171	21444	13151	232	232	159,80	19,93	50,00	50,00
97	Convalescent	M	1086	25681	6177	232	296	201,80	13,49	50,00	50,00
98	Convalescent	M	2751	18042	10467	232	327	155,70	49,73	50,00	1011,94
99	Convalescent	F	1877	24491	7723	232	232	97,20	4,09	50,00	214,50
100	Convalescent	F	720	9995	3355	232	351	66,59	14,12	114,35	73,75
101	Convalescent	M	1299	12623	7128	232	232	25,44	8,07	50,00	50,00
102	Convalescent	F	1309	8246	5663	232	232	31,52	4,25	50,00	50,00
103	Convalescent	F	637	4335	2877	232	232	7,81	4,09	106,09	385,36
104	Convalescent	M	930	4893	6456	232	232	47,88	4,09	50,00	50,00
105	Convalescent	M	481	3878	1729	232	247	10,29	4,57	52,77	196,23
106	Convalescent	F	1883	14455	4195	232	232	100,70	4,09	56,40	84,53